T-2833

Chromatographic Phenomena in Base Leaching of Zinc Oxide

by

Patrick Lamey

T-2833

A thesis submitted to the Faculty and the Board of Trustees of the Colorado School of Mines in partial fulfillment of the requirements for the degree of Master of Science (Chemical and Petroleum-Refining Engineering).

Golden, Colorado

Date January 6, 1986

Signed Patrick Lamey

Patrick Lamey

Approved Annette L. Bunge

Annette L. Bunge
Thesis Advisor

Golden, Colorado

Date 1/6/86

Arthur J. Kidnay, Head
Department of Chemical
Engineering and Petroleum
Refining

ABSTRACT

The base leaching of zinc oxide with either ammonium leaching solutions or sodium hydroxide solutions was examined. A packed column containing a zinc oxide and sand mixture was subjected to either of the leaching solutions and the zinc concentration and pH profiles were measured. Parameters examined were flow rate and lixiviant concentration. Chromatographic models were developed to describe the observed phenomena qualitatively.

Table of Contents page

List of Figures page

page

page

List of Tables page

Acknowledgements

I would like to acknowledge the National Science Foundation for their financial support of this project under grant number CPE-8205238. In addition, I would like to thank Dr. A. L. Bunge for her guidance throughout this project.

Chapter 1
INTRODUCTION

In-situ leaching and heap leaching are alternatives to open pit or deep shaft mining for the recovery of metals. In-situ leaching has been gaining use and interest because of its minimal disturbance of the surface environment. The process of in-situ leaching (or solution mining) entails injection of leaching solution (lixiviant) into an ore body by a series of drilled wells. The leaching solution then dissolves the surrounding rock and complexes the desired metal. The pregnant liquor containing the complexed metal is recovered at the surface where it is processed. In processing, the complexed metal is extracted. The extracted leaching solution is filtered and then returned to the field where it is re-injected into the ore body. Figure 1 shows an idealized in-situ leaching operation.

Commercial operations of in-situ leaching have been, to date, restricted to the recovery of uranium. Uranium is an ideal candidate for recovery by in-situ leaching mining techniques because of the inherently low percentage of uranium in its occuring ores. Because of the small amount of uranium present in the ores, it becomes necessary to move vast amounts of these ores to recover commercial

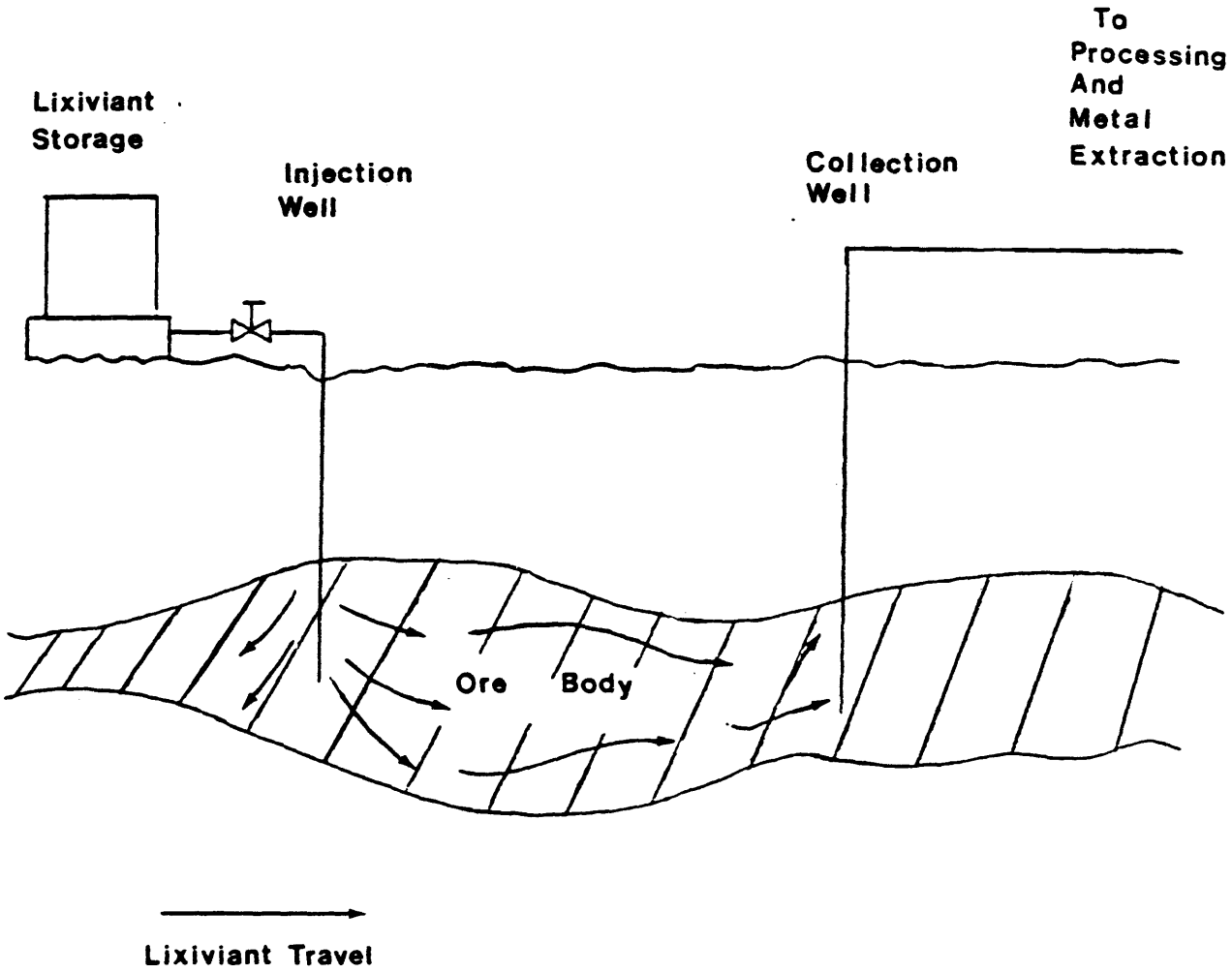

Figure 1

Idealized In-Situ Leaching Operation

quanities of yellowcake (U_3O_8). This increases both capital costs and operating costs for a conventional mine in the business of recovery of uranium. One such commercial operation utilizing in-situ leaching technology for the recovery of uranium is Mobil Corporation's El Mesquite, Texas facility. This particular facility produced more than 295,000 kgs of yellowcake per year at peak operation. However, slackening demand for yellowcake uranium has mothballed the El Mesquite operation. This decrease in demand is due primarily to the fact that no new nuclear power plants have been ordered in the U.S. since 1979. This, in turn, has affected research related to the in-situ extraction of uranium. However, there is a large accumulation of data of in-situ leaching technology in general because of this research.

In-situ leaching and heap leaching are very similiar. In actual use, several or more metals may be grouped in the ore body or heap. The leaching solution itself will be in equilibrium with some of the constituents of the ore or heap and not in equilibrium with other constituents. Also, the mechanisms by which the metals find their way into solution are similiar. Given this, data obtained from in-situ leaching systems will be applicable toward heap leaching systems.

The current push in in-situ leaching research is now focusing in the area of the recovery of the primary metals, copper, lead, and zinc. These metals are of interest because the ore bodies containing them are deteriorating in quality and hence cost of extraction is escalating. However, this effort is tempered to some degree because of stagnating prices for these metals on world markets. Therefore, companies are less willing to expend financial resources to research and develop a new technology. Heap leaching is being utilized primarily in the recovery of gold and silver. It is also being used to recover copper by bacterial leaching methods.

The object of this research was to study chromatographic phenomena in a selected model system. The system selected as the model for this study was zinc oxide (hexagonal) mixed with quartz as the gangue material. Although this system has no practical industrial interest, it was chosen because of its relatively simple solution chemistry. Zinc oxide does not require a two step dissolution process (i.e. oxidation and complexation) nor does it form a large number of species in solution.

Zinc was leached with either high pH ammonia or sodium solutions. Zinc solubility is influenced by the soluble species which form at different pH values. In particular,

complexes with ammonia are responsible for much of the enhanced zinc solubility in ammonia solutions. The speciation of dissolved zinc and ammonia will vary with pH. These species are calculated by combining electroneutrality and material balances with equilibrium expressions for the various reactions. Details of these calculations are given in Appendix A.

Figure 2 shows zinc speciation when no ammonia is present. The expected trends are observed. In low pH solutions, the divalent cationic species dominates; while the anionic species dominates at high pH.

Figures 3 through 6 show species calculation when ammonia is present at four different concentrations. These concentrations of total ammonia correspond to the four solutions used in this study. Table 1 summarizes the chemistry of these lixiviants. The total zinc concentration values used were those obtained from column runs using those lixiviants. When ammonia is present, the $Zn(NH_3)_3^{2+}$ species is the predominant complexed form of zinc. In the high concentration ammonia solutions (Figures 3 and 4), the $Zn(NH_3)_3^{2+}$ form is for all purposes the only zinc species over a considerable pH range. In the lower concentrations (Figures 5 and 6), the $Zn(NH_3)_3^{2+}$ form is a much smaller peak and covers a smaller pH range. In all cases, the zinc

ammonia complex causes shifting of the other species curves.

Table 1 shows the expected equilibrium speciation for the four leaching solutions studied in this research. In comparing the two ammonium leachants, the 0.25 M ammonium hydroxide with no salt addition was chosen because the ammonium ion concentration was thought to be roughly the same as the 0.15 M ammonium hydroxide / ammonium nitrate leachant. However, as shown in Table 1, this was not the case. If this had been so, it would have been possible to examine the effect of pH on the solubility of zinc oxide at fixed ammonium ion concentration.

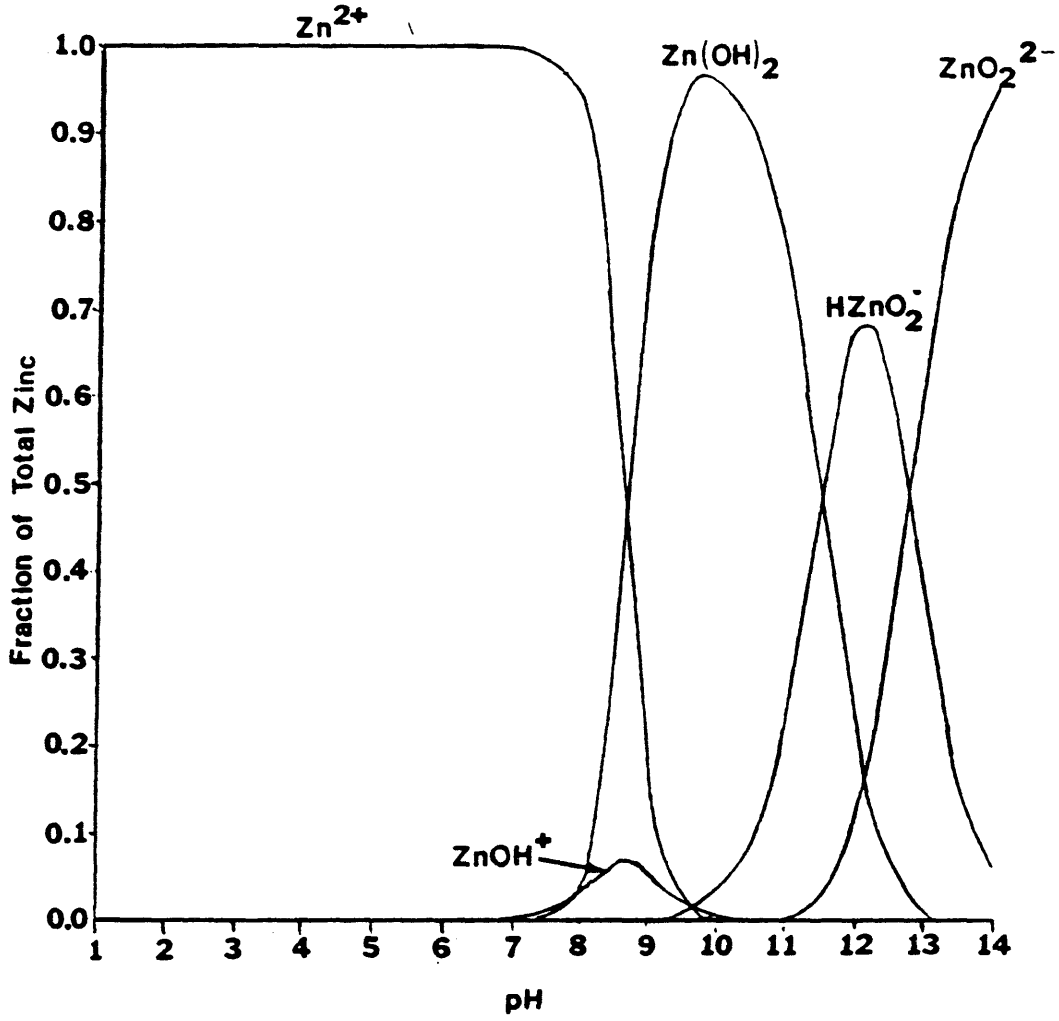

Figure 2

Zinc Species as a Fraction of Total
Zinc as a Function of pH at 25 C

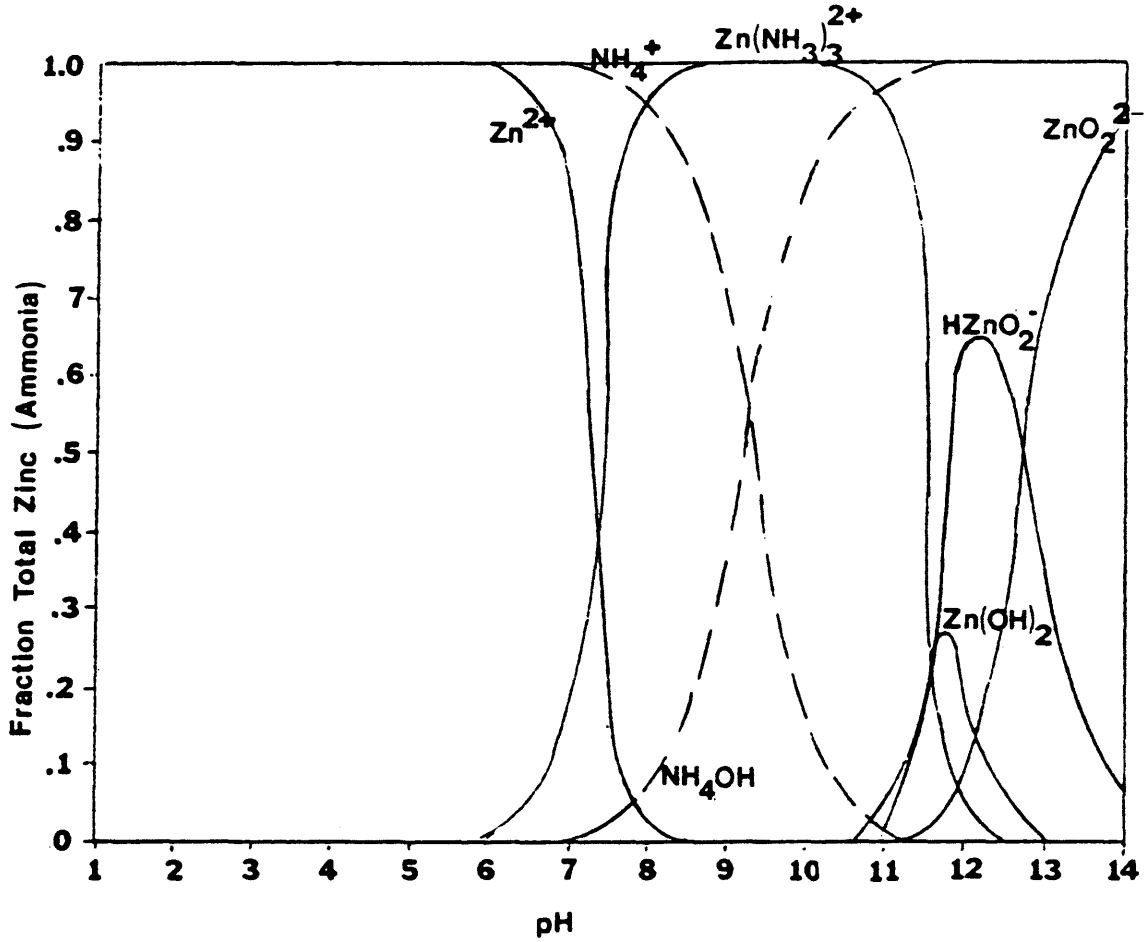

Figure 3

Fraction of Zinc Species and Ammonium Species as a Function of pH for a Total Ammonia Concentration of 0.155 M (25 C) Total Zinc Concentration of 20 ppm

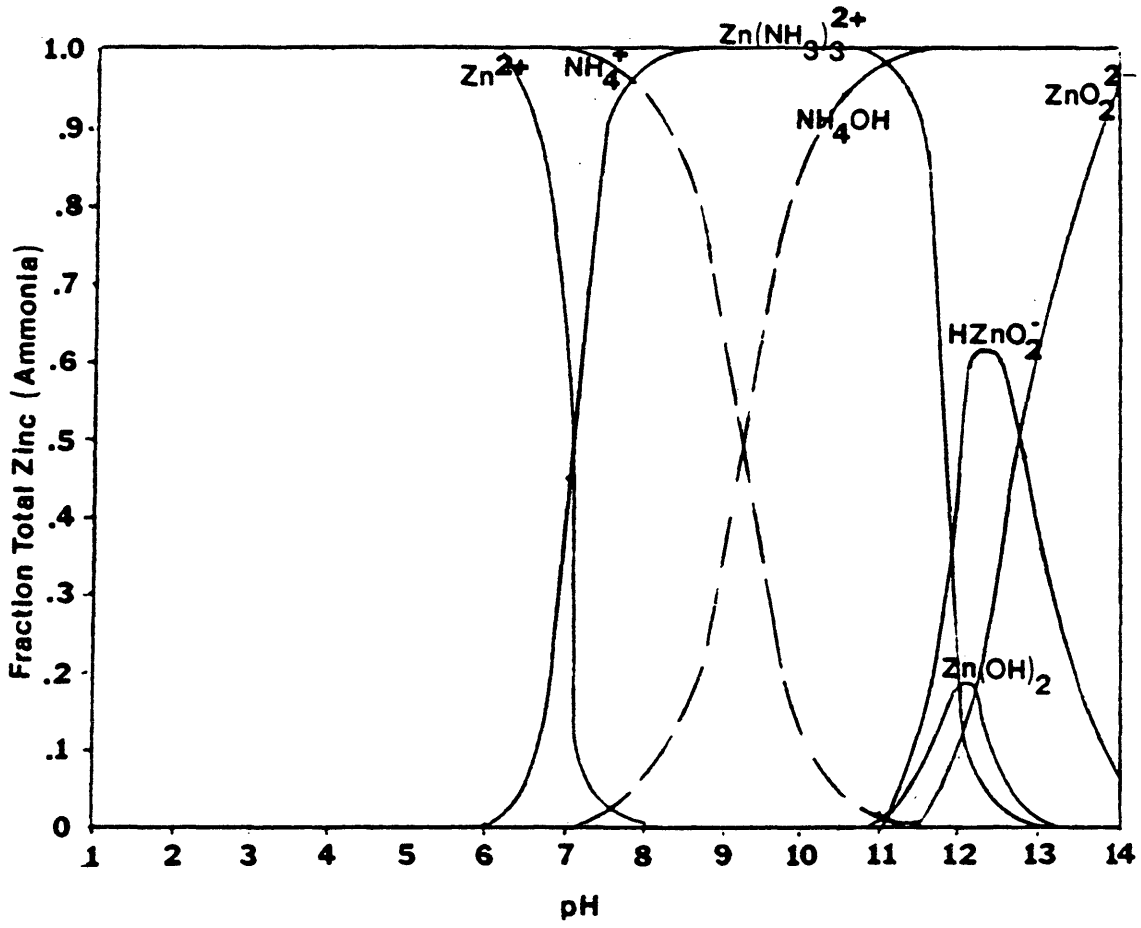

Figure 4

Fraction of Zinc Species and Ammonium Species as a Function of pH for a Total Ammonia Concentration of 0.25 M (25 C) Total Zinc Concentration of 25 ppm

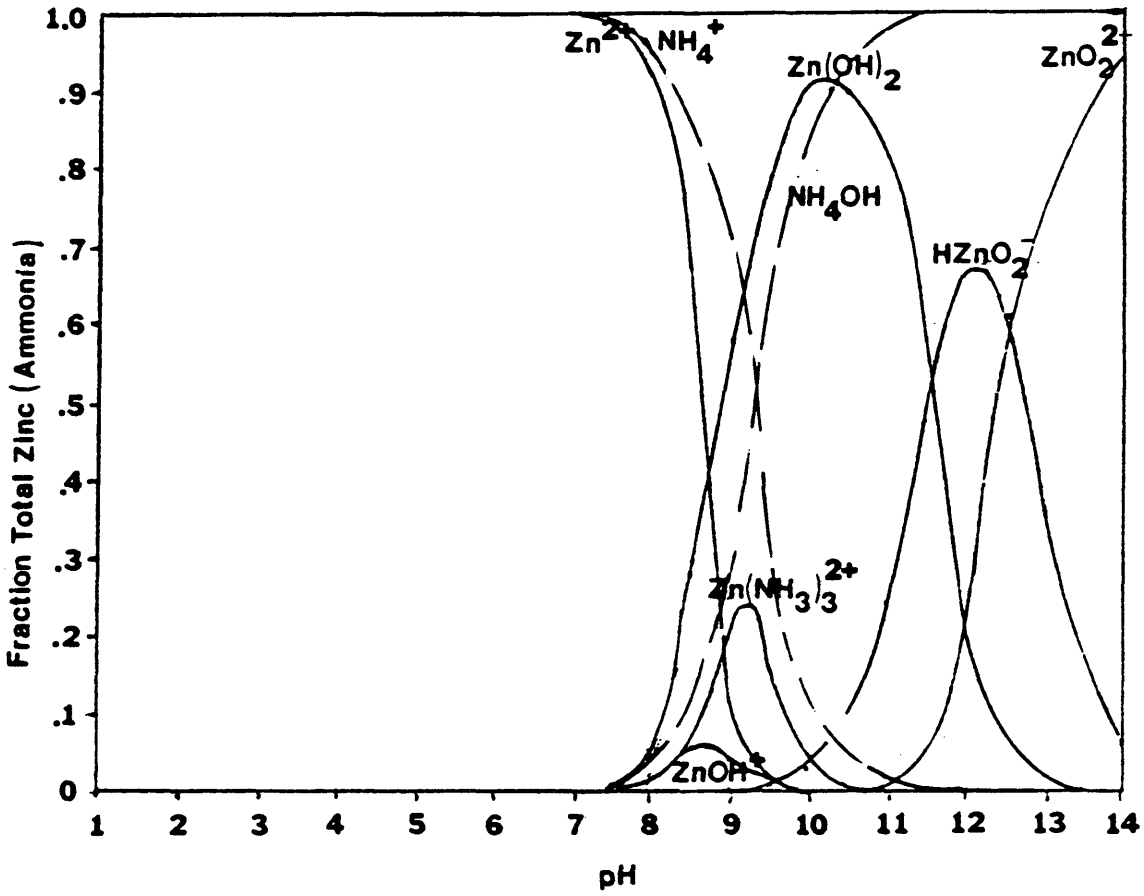

Figure 5

Fraction of Zinc Species and Ammonium Species as a Function of pH for a Total Ammonia Concentration of 0.005 M (25 C) Total Zinc Concentration of 4 ppm

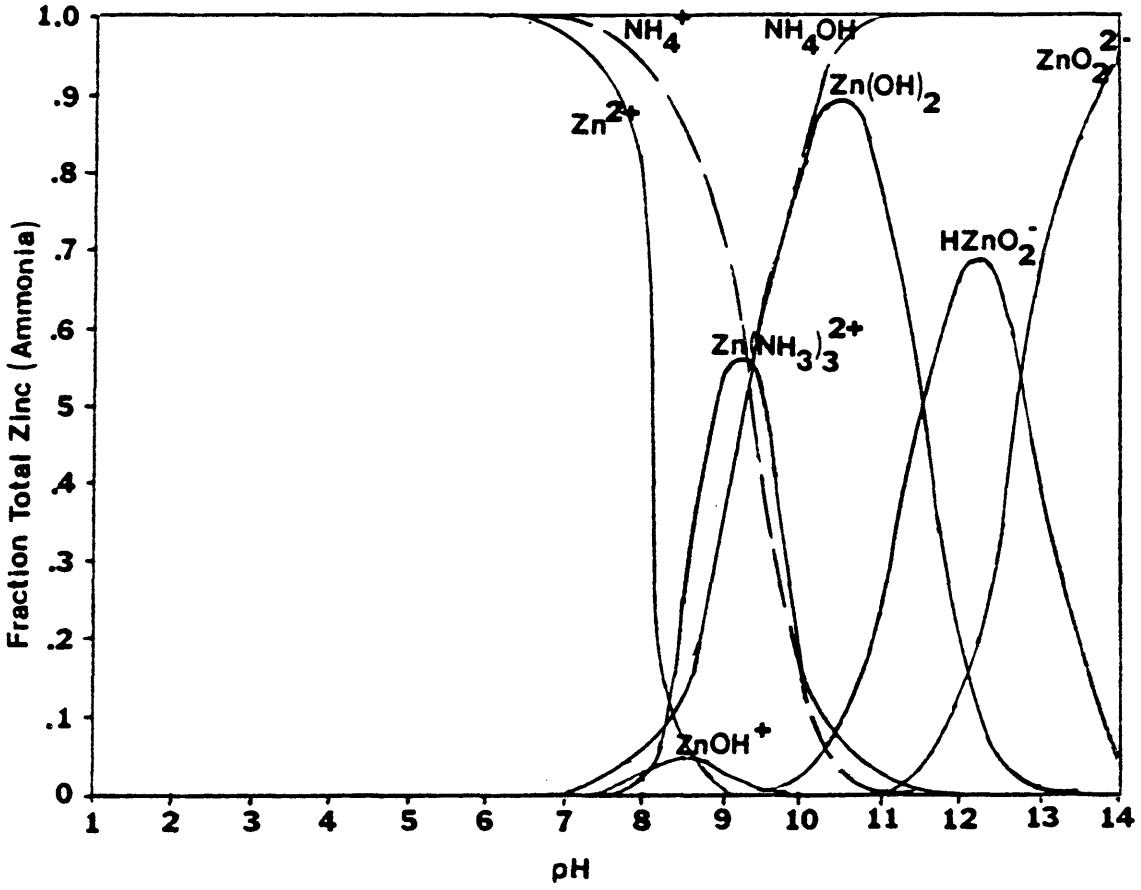

Figure 6

Fraction of Zinc Species and Ammonium Species as a Function of pH for a Total Ammonia Concentration of 0.008 M (25 C) Total Zinc Concentration of 2 ppm

Table 1

Expected Equilibrium Speciation for
Leaching Solutions at 25 C
(Based on Calculations in Appendix)

Lixiviant	Na^+ (M)	NH_4OH (M)	NH_4^+ (M)	OH^- (M)	pH
0.15 M ammonium hydroxide/0.005 M ammonium nitrate	-	.149	4.94×10^{-3}	5.43×10^{-4}	10.7
0.25 M ammonium hydroxide	-	.247	1.80×10^{-3}	2.47×10^{-3}	11.4
0.01 M sodium hydroxide/0.005 M ammonium nitrate	.01	4.98×10^{-3}	1.80×10^{-5}	4.97×10^{-3}	11.7
0.01 M sodium hydroxide/0.008 M ammonium nitrate	.01	4.96×10^{-3}	4.39×10^{-5}	2.03×10^{-3}	11.3

Chapter 2
LITERATURE REVIEW

In compiling this selected literature review, documents examined regarding the chemistry of in-situ leaching were not restricted to that of zinc oxide. Because of the scarcity of material related directly to zinc oxide, whether solubility data or otherwise, a broad review encompassing uranium and other metals was merited. Therefore, this review has been divided into several sections: uranium leaching, copper leaching, and zinc leaching. Because the overall intent of the project is to understand leaching processes, this review of other systems is appropriate.

Uranium Leaching Chemistry

Uranium extraction by in-situ methods can be divided into two different areas: alkaline and acid. The alkaline leaching of uranium is by far the more predominant. The alkaline leaching of uranium has been dominated by carbonate / bicarbonate chemistry. Batch and column test data has been collected for the leaching of uranium ore found in the Crownpoint, New Mexico deposit (Vogt, et al.,

1982). The lixivaint used was sodium bicarbonate with oxygen or hydrogen peroxide as the oxidant.

In this system, the uranium in the ore is oxidized by the oxygen or hydrogen peroxide and then complexed with the free carbonate ions in the lixiviant. Once complexed, the uranium remains in solution. Using a flow rate of 0.2 pore volumes per day (i.e., 10 days for the solution to pass through the entire pore volume in the sample), recoveries of 60% to 95% by weight of the ultimate amount of uranium available were obtained after 96 hours in column tests.

Batch tests were done in conjunction with the column tests to determine ultimate solubility of uranium in the lixiviant. Uranium recoveries in the batch tests were 40% to 95% by weight of the ultimate amount of uranium available.

The investigation found that using either oxygen or hydrogen peroxide as an oxidant made no difference in rate of recovery or amount of recovery in the same type sample. This confirmed earlier work (Litz, 1982) on the comparison of oxygen and hydrogen peroxide as oxidants in sodium bicarbonate leaching solutions for uranium.

Vogt, et al. (1982) found rate and amount of recovery were influenced most by the mineralogical make-up of the sample. All samples used in this evaluation were

sandstone with the uranium occuring as coffinite (with carbonaceous material) or uranite. The uranite tended to have higher leach rates than that of the coffinite. The data indicated that the carbonaceous material "shielded" the uranium and thus kept the rate low. The chemistry used in this evaluation was based upon a patent by Habib and Vogt (1978). Further research on these alkaline systems has included study of the consumption of the oxygen in ammonium bicarbonate / oxygen lixiviants for uranium in sandstone (Goddard and Broshahan, 1982).

Along these same lines, Walsh, et al. (1979) examined the migration and displacement of the ammonium ions from uranium leaching sites in an ammonium bicarbonate / hydrogen peroxide system. During solution mining, the ammonium ions occupy and finally saturate the mineral exchange sites. Removal of these ions from the uranium bearing rock is important from an enviromental point of view. By using a mathematical model, the investigators evaluated the effect of cation composition and concentration of the displacement solution, including dispersion effects, on the overall effectiveness of the solution to displace ammonium ions. The results of the study indicated that by increasing the concentration of monovalent ions in a solution containing both monovalent and divalent ions, high selec-

tivity toward displacement of the ammonium is achieved. Even after the majority of the ammonium ions have been displaced by the restoring solution, what remains tends to migrate as a result of incoming ground water flux.

Experimental work along these same lines has included research on the displacement of ammonium ions by sodium hypochlorite (Paul, et al., 1981). This report indicated that the sodium hypochlorite is effective in removing the ammonium but its consumption rate is high due to the high number of side reactions. These include iron sulfide oxidation and molybdenum sulfide oxidation.

The acid leaching of uranium ores is coming under increasing study. Nigbor, et al. (1982), actually compiled a case history for in-situ sulfuric acid leaching of uranium for a pilot scale facility. This evaluation ran for more than two years. The data showed that the sulfuric acid was an effective leaching agent. Using 3 to 5 grams of lixiviant per liter of ground water, recovery in the production solution was typically 80 to 100 ppm uranium. Site restoration was successful but required extensive flushing. The pH took 350 days to return to its baseline level.

A number of patents have been granted in the area of acid leaching of uranium. For example, Martin (1978) was

granted a patent for a sulfuric acid and peroxomonosulfuric acid system. The peroxomonosulfuric acid served as the oxidant.

Copper Leaching

Carnahan (1982) conducted research to determine the effect of temperature on the sulfuric acid / oxygen leaching of chalcopyrite ore. As in the case of uranium leaching with carbonate solutions, the copper is oxidized by the oxygen and complexed with the sulfate ions. Experimentation was conducted at 35 C and 90 C. Using batch charges and an excess of lixiviant, oxygen pressure was maintained at 400 psig. At 90 C, 47% by weight of the available copper was extracted after 913 days. At 35 C, 27% of the available copper was recovered after 915 days. The rate of leaching was controlled by diffusion of lixiviant into and out of the ore fragments. Oxygen consumption at 90 C was more than twice that of 35 C. In addition, sulfuric acid consumption at 90 C was 40% greater than the consumption at 35 C.

Parallel with this work, Carnahan and Lindstrom (1982) investigated the effects of sodium chloride upon the recovery of copper using the same leaching system. Again

using a batch apparatus and the same leaching conditions, the recovery of copper from the ore was enhanced by the addition of sodium chloride to leaching solution. At 90 C, 67% by weight of the available copper was recovered in 1236 days as opposed to 47 % extracted at 90 C without the sodium chloride addition. The consumption rate of oxygen was not greatly affected by the addition of sodium chloride.

Attempts have been made to compare models with actual leaching data for the recovery of copper from copper oxide ore using sulfuric acid (Schafer, et al.). The copper in the ore was primarily in oxide forms with a minimum of sulphides which were not of the chalcopyrite form. Good correlation between experimental data obtained during column leaching of course ore and the predicted behavior of the shrinking core model was obtained. However, attempts to model all aspects of the observed phenomena failed. It was hypothesized by the authors that the particle size distribution played a key role in determining the actual flow rates of leachant through the ore and hence recovery.

Zinc Leaching

Venkataswamy and Khangaonkar (1981) examined the leaching of sphalerite (primarily zinc sulfide) with ferric chloride and tetrachloroethyelene. The tetrochloroethyelene was added to the lixivaint to prevent deposition of elemental sulfur on the sphalerite particles. If this deposition is allowed to occur for a long enough period of time, the leaching rate eventually becomes diffusion limited. By using the tetrachloroethyelene, 95% by weight of the available zinc was recovered over 7 hours as compared to 65% recovered over the same period of time without the tetrachloroethylene. Increasing the ferric chloride concentration yielded slight enhancement of zinc recovery. At 3 M, the yield was 67.8% while at 4 M, the yield was 68.6%.

Further work has been done on the leaching of sphalerite by ferric chloride systems (Dutrizac and MacDonald, 1978). The system used in this research was a ferric chloride and hydrogen chloride system. The system was evaluated at temperatures ranging from 25 C to 100 C. Hydrogen sulfide was formed at high concentrations of hydrochloric acid (greater than 1 M). The recovery of copper and rate of recovery were enhanced by increased

hydrochloric acid concentration.

In the case of zinc oxide leaching, most of the work has been involved with the reclamation of zinc from various smelting residues and very low grade zinc oxide ores. One such investigation involved the leaching of oxidic zinc materials by chlorine and chlorine hydrate. Processing for the leaching occurred in the batch mode. This particular evaluation leached a variety of various zinc oxide residues and compared the degree of recovery. In addition, the investigators matched the leaching behavior of Electric Arc Furnace dust to a shrinking core model.

Jones and Klaman (1953) examined the solubility of zinc oxide in aqueous solutions of ammonium hydroxide / ammonium salts as a function of pH. Their research indicated that there was enhanced solubility of zinc oxide in solutions of ammonium hydroxide / ammonium salts when compared to solutions of the same pH using potassium hydroxide.

Chapter 3

EXPERIMENTAL APPARATUS AND PROCEDURE

Experimental Apparatus

The experimental apparatus used in this project consisted of the following components: a stainless steel column packed with a mixture of sand and zinc oxide, a high pressure liquid chromatography (HPLC) pump to deliver either water or leaching solution to the column, and a fraction collector to retain column effluent for later analysis. The entire system is shown in Figure 7.

Instruments used in this evaluation included a pH meter to monitor changes in the column effluent, an on-line conductivity cell and associated meter to monitor changes in solution conductance, an on-line differential refractive index (RI) detector, and an Instrumentation Laboratory IL-951 Atomic Absorbence Unit to measure the zinc present in the column effluent. System units were interconnected by either 1/16-inch stainless steel tubing (0.005 inch ID) or by teflon tubing with a 1/8-inch OD. The solutions were kept in two gallon Nalgene vessels. The HPLC pump drew a solution from one of the reservoir vessels through a five micron stainless steel submersible cartridge filter via the

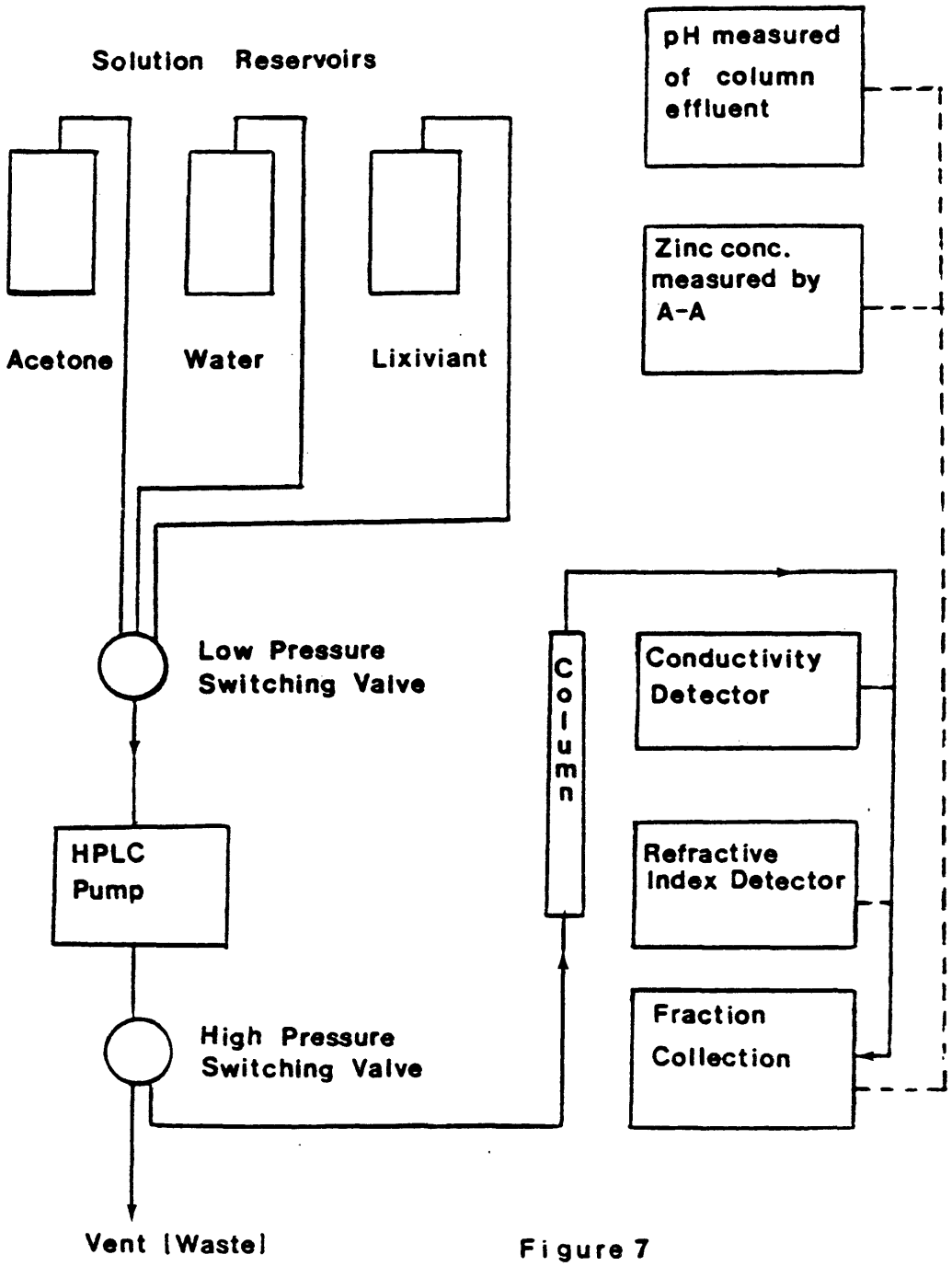

Figure 7

Schematic of Apparatus

1/8-inch teflon tubing to a teflon switching valve on the low pressure (inlet) side of the pump. This valve can accommodate up to six different solutions for selection to a single outlet, i.e. flow to the HPLC pump.

HPLC Pump

The HPLC pump used in this project was a Beckman model 112. Pumping action was provided by a single reciprocating piston made of sapphire. Because of rapid refill and the backpressure of the packed column, pulsing of solutions was minimal. A calibration curve was generated to correlate pump LCD readout flow rates against actual flow rates obtained during operation. This line is shown in Figure 8. According to the manufacturer, flow rate reproducibility is ± 0.3% (or 0.003 mL/min, depending upon which is greater) and flow rate accuracy is ±1.0%.

Column

Once the pump delivered solution through the outlet check valve, the flow continued on to a high pressure switching valve. This valve was constructed of 316 stainless steel with a Tefzel rotor. The valve switched

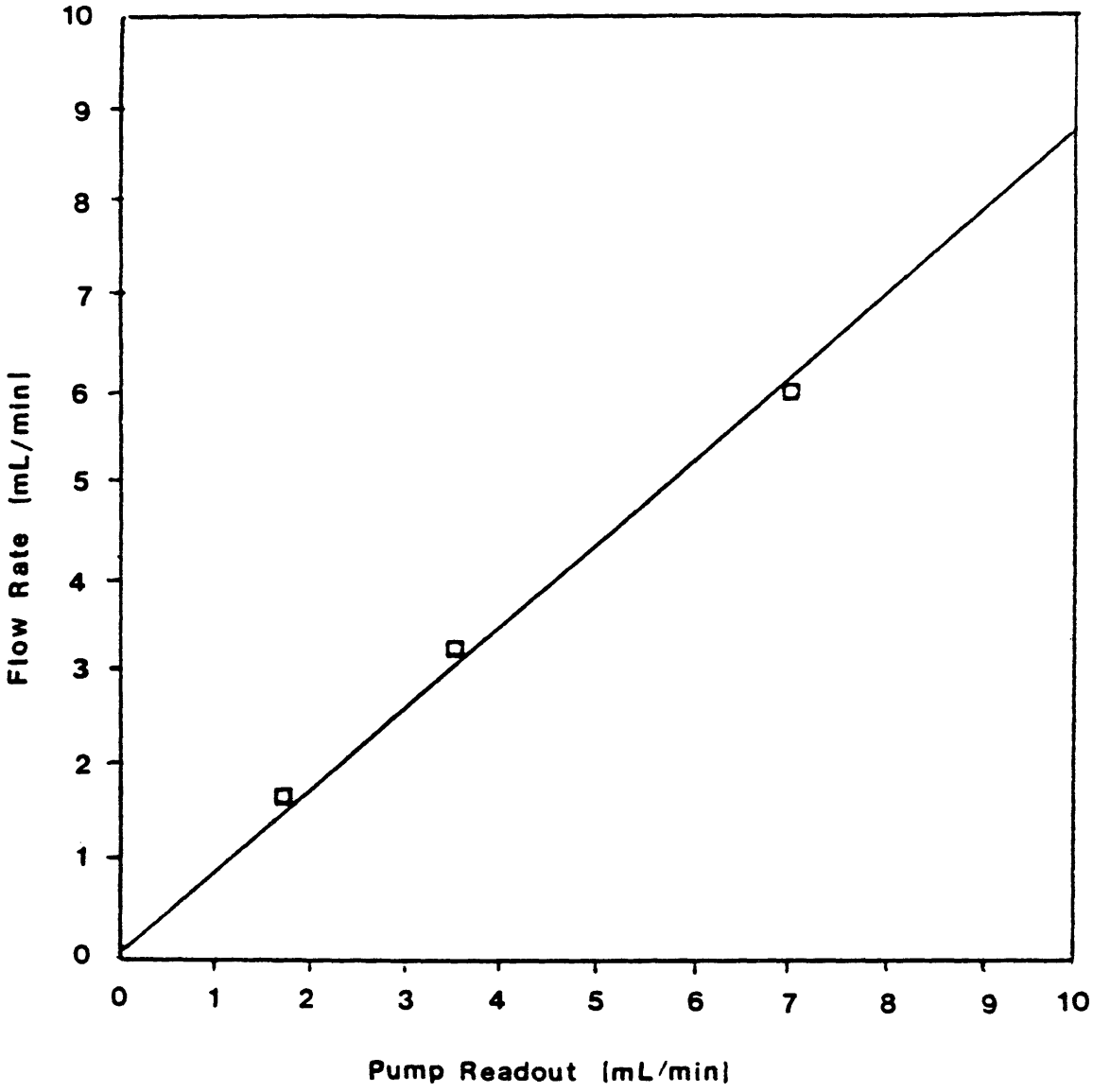

Figure 8

Flow Rate Versus Pump Readout

the flow exiting from the pump to either the vent (waste) line or to the inlet of the column. The column itself was fabricated of 1/2-inch 316 stainless steel tubing. It measured 0.402 inches ID (1.02 cm) and 24 inches (60.96 cm) in length. This gave the column an internal volume of roughly 50 cubic centimeters. The tubing itself had a burst pressure of better than 14,000 psi which was adequate for flow rates with sustained pressure drops of 4,000 psi or better. The column was fitted with 1/16-inch to 1/2-inch reducing unions to make interconnection with the rest of the system. A 0.4 micron 316 stainless steel frit was incorporated at each end of the column to prevent any small particles (>200 mesh) from exiting the column and damaging any of the on-line downstream instruments or plugging the outlet tubing. Figure 9 shows the column.

Fraction Collector

The fraction collector was located at the end of the experimental apparatus, following the on-line instruments (conductivity cell and refractive index detector). The instrument used in this case was the ISCO model 1850 Fraction Collector. Each test tube was in turn moved to the collection point beneath the drop former and filled with

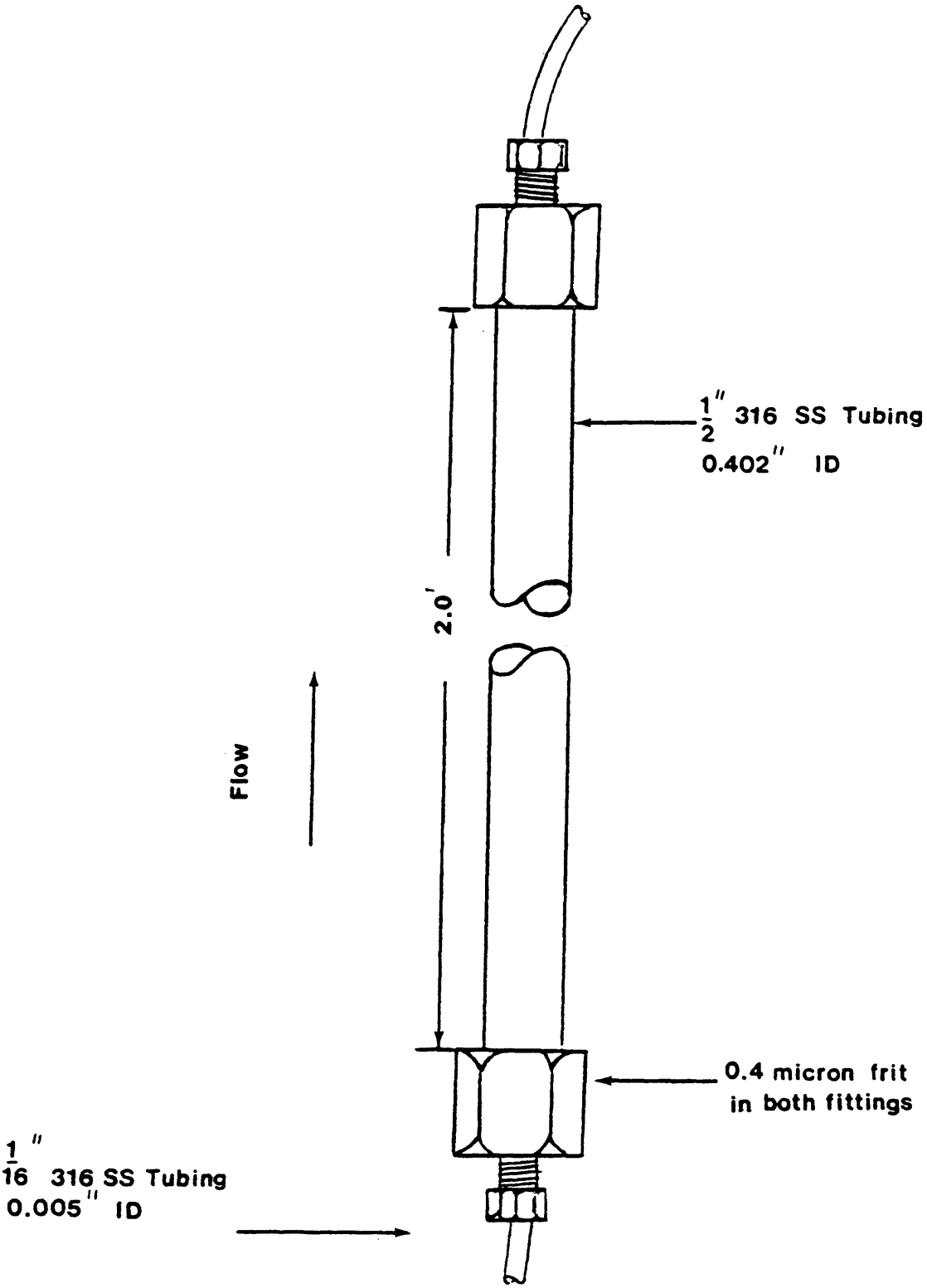

Figure 9

Diagram of Column

typically one to two mL of column effluent.

Experimental Procedure

Sand and Zinc Oxide Preparation

As mentioned earlier, the packing used in this column was a mixture of sand and zinc oxide. The sand itself was purchased from the Cherry Creek Sand Specialties Company of Denver, CO. As initially bagged, it was for the most part 20 to 40 mesh. The sand was ground in an impact crusher. This impact crusher is shown in Figure 10. Approximately 200 grams were placed in the impact crusher. The crusher was then turned on and the sand ground for roughly 3 to 5 minutes. The resulting sand particles were then separated using stainless steel screens. Once this separation was accomplished, each particular range of particle size was stored in tightly capped flasks.
The zinc oxide used in this project was donated by the St. Joe Resources Company of Monaca, PA. The zinc oxide used was their 922 Zinc Oxide hard granules, lot no. 322004. This was 99.8% pure zinc oxide which was manufactured using the French Process. The resulting product has a very low percentage of impurities. The French Process yields

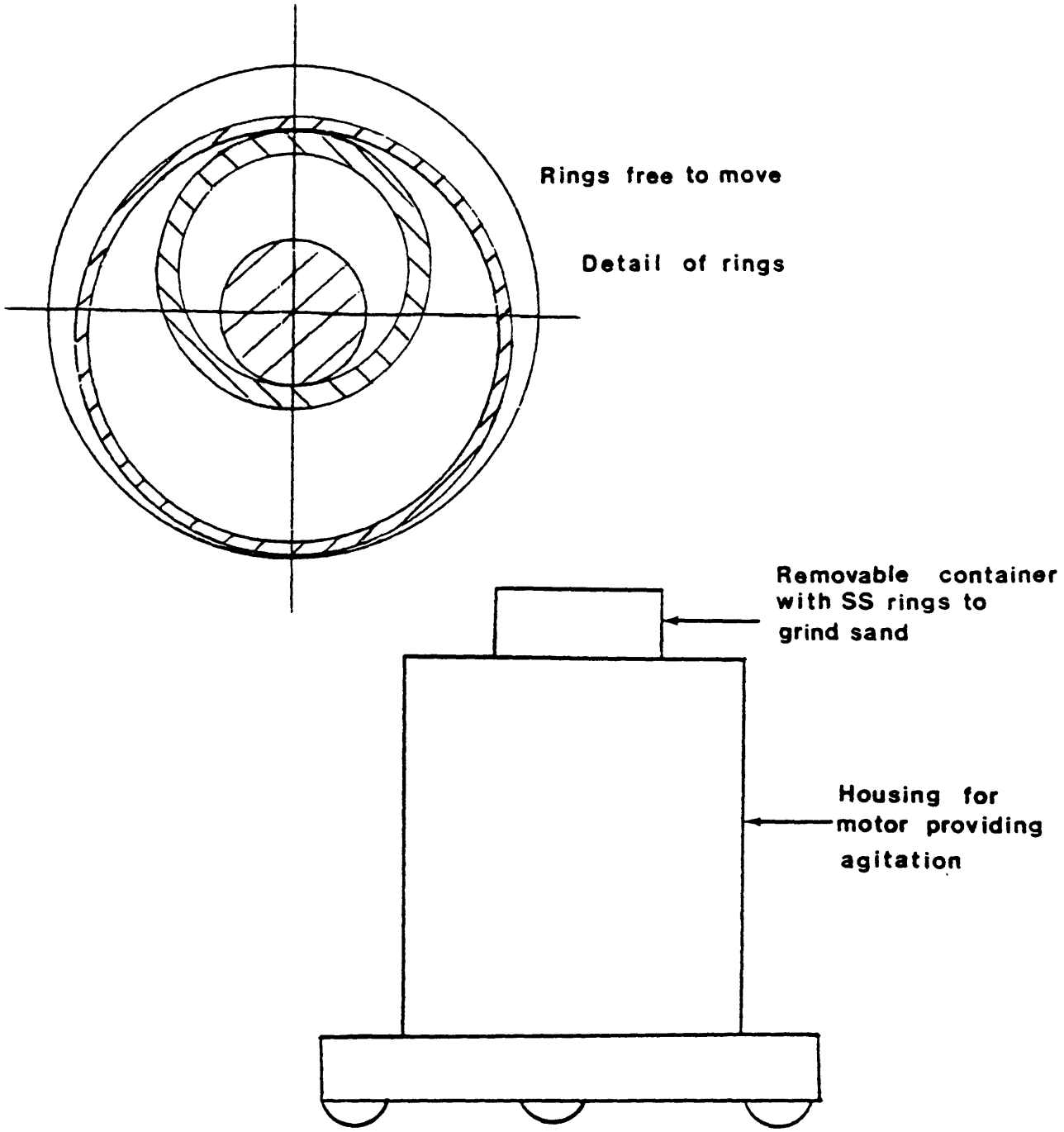

Figure 10

Diagram of Impact Crusher

zinc oxide by oxidizing high purity, double distilled metallic zinc vapor. The particles formed are 0.1 to 0.4 microns in diameter. These resulting particles are then calcined at 600 C and processed through a granulator to yield particles roughly 10 mesh in size.

The zinc oxide from St. Joe's was prepared for use in the column by sintering it in a muffle oven at 600 C for 24 hours. This was done to harden the granules prior to grinding. The granules are of a yellow color immediately after removal from the muffle oven. The granules regain their white color as they cool. The granules were then ground using a mortar and pestle. The resulting zinc oxide particles were then screened to the same mesh distribution as that of the sand. The zinc oxide was also kept in tightly capped flasks.

Column Packing

The column used in all runs was packed with a mixture of 10% by weight zinc oxide and 90% by weight sand. The zinc oxide and sand mixture was made in batches of 100 grams (90 grams of sand and 10 grams of zinc oxide). The 90 grams of sand had the following mesh distribution by weight:

10% 28-48 mesh	20% 100-150 mesh
20% 48-65 mesh	20% 150-200 mesh
20% 65-100 mesh	10% >200 mesh

The 10 grams of zinc oxide, however, was restricted to the 65-100 mesh range. The weight for each fraction was measured to the nearest ± 0.01 grams on Mettler PN2210 balance. The fractions were then combined and thoroughly mixed.

The column with fittings and associated frits was then weighed to the nearest 0.01 grams. The zinc oxide and sand mixture was then spooned into the open end of the column in small amounts of roughly 2 to 3 grams. The mixture was settled by repeated tapping. Once the column was full, the fitting and associated frit were reattached to the column. The column was then reweighed to the nearest 0.01 grams. The mass of the sand and zinc oxide was then determined by difference.

Determination of Void Fraction

After the column was packed, it was saturated with water to determine its void volume. The water itself was the purified product of a Milli-Q Water Purification System manufactured by the Millipore Corporation. The system

consisted of an activated charcoal filter, an organic removal filter, and two deionization cartridges.

Water was pumped through the column at a flow rate of 0.05 mL/min for a period of 48 hours. The column outlet was attached to a vacuum pump with a draw of -20 inches of Hg vacuum. A cold trap was placed between the column outlet and the pump to prevent any condensation within the pump. The set up for this procedure is shown in Figure 11.

After the 48 hours, the column was separated from the rest of the system. Careful examination was then made of the packing at each end of the column. At the column outlet, the packing was examined to check for any possible accumulation of particle fines. At the inlet, a check was made to see if there had been any additional compaction of the column packing due to the water saturation process. If this were to occur, the calculation of the void volume would be inaccurate. If no packing compaction was observed, the column was then reassembled and weighed. The difference in the column weight after saturation and the column weight before saturation represents the mass of water occupying the column's void volume.

All runs were done at a temperature of 25 C. Given this, a density of 1.00 g/mL was selected for water. As the column was weighed to only the nearest 0.01 g, a more

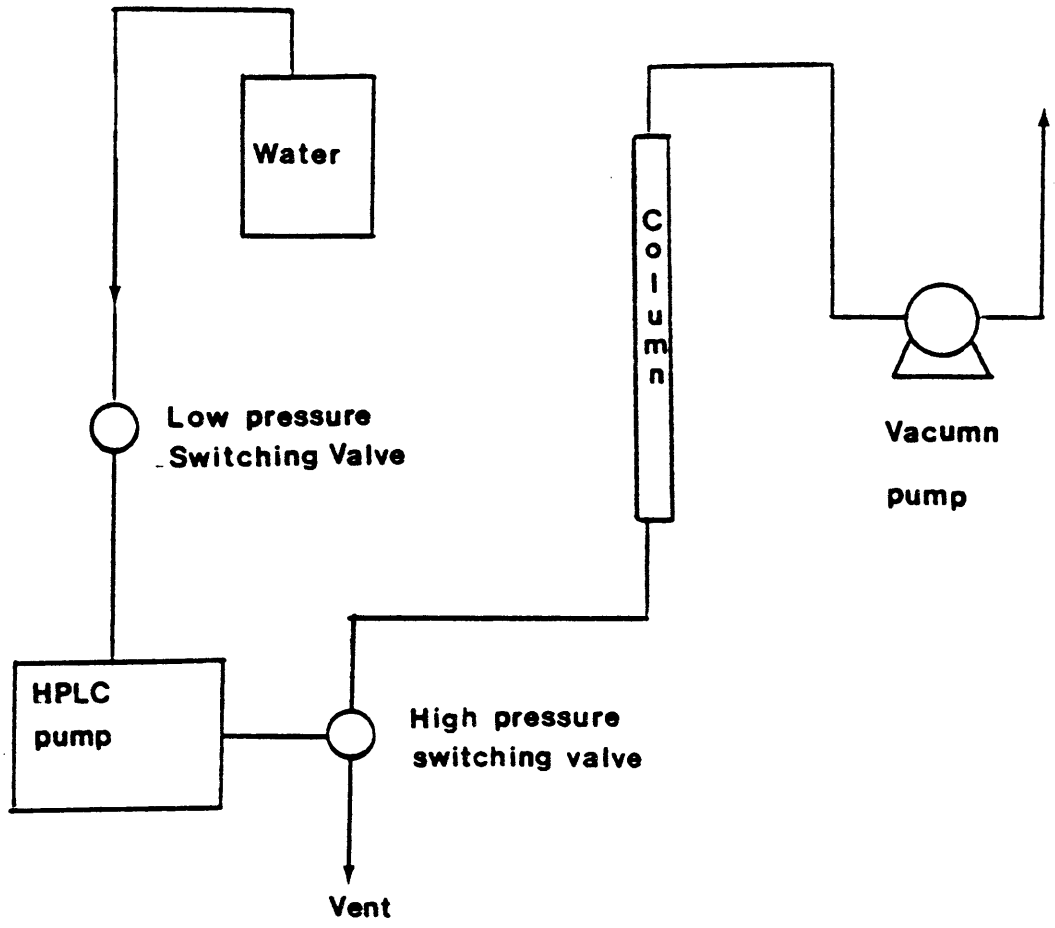

Figure 11

Apparatus for Column

Saturation by Water

accurate density value was deemed unnecessary. The void volume is easily calculated and hence the void fraction, ϵ, which is the volume of the water divided by the total volume of the column.

Solution Make-up and Preparation

All solutions were vacuum filtered through a 0.45 micron filter prior to use. By using vacuum filtration, any fine particulate present in the solutions was eliminated. In addition, the solutions were degassed so as to prevent bubble formation in the lines or in the pump piston. The leaching solutions were, after filtration, measured for pH.

pH Meter Calibration Before Use

In calibrating the pH meter, the temperature control dial on the instrument was set to the ambient temperature. The instrument was then standardized over a working pH range of 4 to 10. The electrode was standardized against the pH 4 standard and the slope control was used to bring the measured value of the pH 10 standard into agreement with its prescribed value at ambient temperature. The pH 4

standard was again measured and the electrode re-standardized. This was repeated until both standards were correct on the meter readout.

Cleaning Treatment for New Test Tubes

Prior to using any test tubes for the first time, a cleaning procedure was followed to prevent contamination of column effluent. The tubes were immersed in concentrated sulfuric acid for a period of 8 hours. The test tubes were then rinsed with the deionized water and allowed to dry in an inverted position. After this initial cleaning, the test tubes were rinsed thoroughly with the deionized water after use and allowed to dry in an inverted position.

Column Flushing with Water Between Runs

Before using the column again after a data run, water was pumped through the column to remove hydroxide ions from the column. Although it was never possible to bring the pH of the column effluent down to that of the incoming water (roughly pH of 6.3), it was possible to get the pH of the column effluent down to a range of 8.5 to 9.0 pH after pumping about 4 liters of water through the column. The

HPLC pump was set at a high flow rate, usually 7.00 mL/min on the pump readout, so that the reduction of the pH of the column effluent could be accomplished as quickly as possible. Once the column effluent pH was in the specified range, the column was once again ready for use.

Setting the Fraction Collector for Use

The volume of the test tubes used in the racks of the fraction collector were roughly 2.2 mL. In using the fraction collector, the time setting (residence time) for each test tube was adjusted so that each would hold roughly 0.10 of a column pore volume (approximately 1.4 mL). In practice, it was possible to obtain values ranging from 0.09 to 0.13 of a column pore volume per tube.

Pumping Leaching Solution Through the Column

Once the parameters for a particular run had been specified and the equipment set for those parameters, the leaching solution was pumped through the column. As mentioned earlier, water was flushed through the column prior to use. The objective when switching from water to leaching solution was to as closely as possible approximate a

step change. This was done by minimizing the dead volume between the high pressure switching valve and the inlet of the column. See Figure 12 for a detail of the switching valve portion of the experimental apparatus. The dead volume between the high pressure switching valve and the column inlet was roughly two microliters. This was estimated by first measuring the length of the 1/16-inch OD tubing from the high pressure valve to the column inlet. The inside diameter of the tubing was known and the dead volume was calculated by using the formula for the volume of a regular cylinder.

To closely approximate a step change, the high pressure valve was switched to vent (waste). The low pressure valve was then set to allow the HPLC pump to draw leaching solution rather than water. Since the dead volume of the pump and the flow rate were known, it was simple enough to calculate how much time must pass until leaching solution would exit from the waste line. By waiting this required amount of time (plus a margin more to insure that leaching solution exits from the waste line), the apparatus was then ready to introduce leaching solution to the column. The high pressure valve is switched to send leaching solution through the column. Simultaneously, the fraction collector was advanced to test tube number one. The carousel

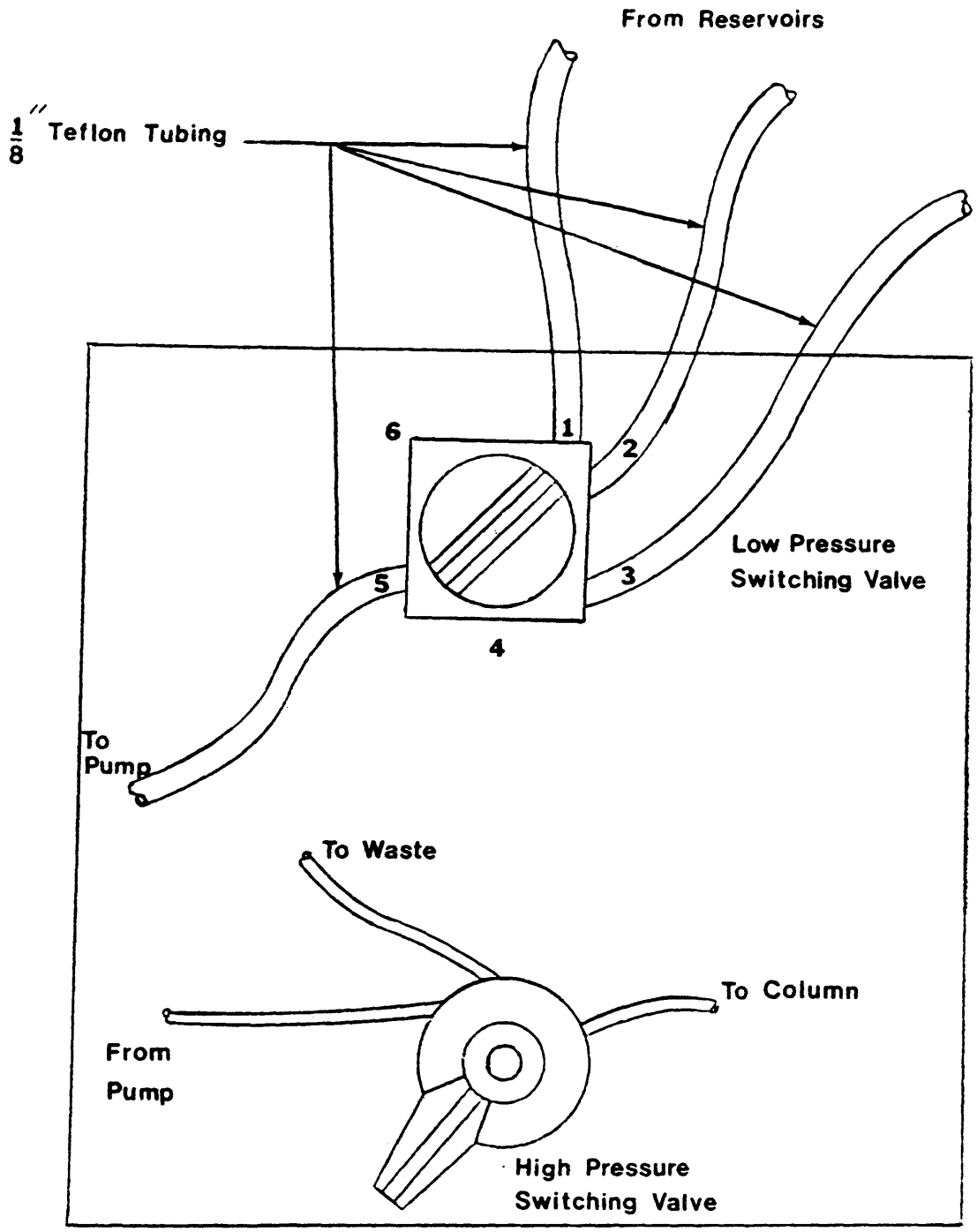

Figure 12
Switching Valves For Experimental Apparatus

advanced each test tube to the collection point under the dropper. Once a run was completed, the effluent from the column was diverted to a waste beaker. The low pressure valve was again set to allow the HPLC pump to draw water and the column was flushed.

Column Effluent Analyses

Once column effluent had been collected for a particular set of parameters, the pH was measured as a function of pore volume. After this pH measurement was done, direct measurement of the zinc in the column effluent was made by atomic absorption. This particular instrument measures zinc over a range of 0.4 ppm to 1.7 ppm. Since the column effluent usually contained more zinc than the specified range, dilution of the samples was necessary.

Samples were taken every 1 pore volume or so, diluted and acidified with 0.5 N nitric acid to a pH of roughly 2, and poured into small polyethylene bottles. Acidifiation was done to insure that all zinc in solution was in the cation form (Zn^{2+}). This was necessary for correct operation of the instruments. Standards were made up over the working range for zinc. Each standard contained the same diluted concentration of ammonium hydroxide and

ammonium salt ions plus the specified amount of zinc. Using the standards, a calibration curve was generated for zinc concentration as a function of absorbence over the working range of the instrument. Based on this calibration curve, the concentration of the zinc in the column effluent was determined.

On-line instruments measured conductivity and changes in the refractive index of the solutions during actual operation. Recorders charted the changes of these two parameters. Samples of the column effluent were saved for later analysis of ammonium ions by cation chromatography.

Ion Chromatography

The column effluent was analyzed for total ammonia using a Wescan model 269-004 cation exchange column. This column was packed with a sulfonated polystyrene / divinylbe-zene cation exchange resin. The column exit was connected to a conductivity cell with data output to a recorder. The elluent for this HPLC column was nitric acid with a pH of approximately 2.5. The elluent flow rate was 1.5 mL/min. Effluent from the zinc oxide/quartz column was diluted by 10:1 with water. The sample size for the standards and zinc oxide / quartz column effluent was 25 microliters.

Bottle Tests

Tests were conducted to determine the ultimate solubility of zinc oxide in the various leaching solutions. In addition, the zinc concentration could be monitored over time. A 125 mL cylindrical beaker was filled with vacuum filtered leaching solution. The solution was then agitated using a magnetic stir bar. At time zero, 1 gram of treated zinc oxide granules (65-100 mesh) or powder (200 mesh) was introduced into the beaker. At given time intervals, a 1 mL sample was withdrawn by syringe. The sample was then passed through a 0.1 micron filter. The solution was diluted with deionized water (50:1) and titrated with 0.01 M EDTA to a colorometric end point using calmagite. End point occurred when the solution changed from red to blue.

Chapter 4
EXPERIMENTAL RESULTS

In studying the alkaline leaching of zinc oxide, two particular systems were examined: an ammonium hydroxide / ammonium salt lixiviant and a sodium hydroxide / ammonium salt lixiviant. For this evaluation, the weight percent zinc oxide in the column was fixed at 10 percent. In addition, the particle size distribution for both the sand and zinc oxide in the column were held constant. Temperature was held constant at 25 C. Lixiviant was pumped through the column at 1.62, 3.13, or 6.26 mL/min.

Bottle Experiments

Results from bottle experiments, given as zinc concentration with time, are reported in Figures 13 and 14 and summarized in Table 2. Although the concentrations of the lixiviants did not match those of the leachants used in the column tests, they were of the same magnitude and qualitative comparison can be made. All zinc samples were powdered unless marked as granular.

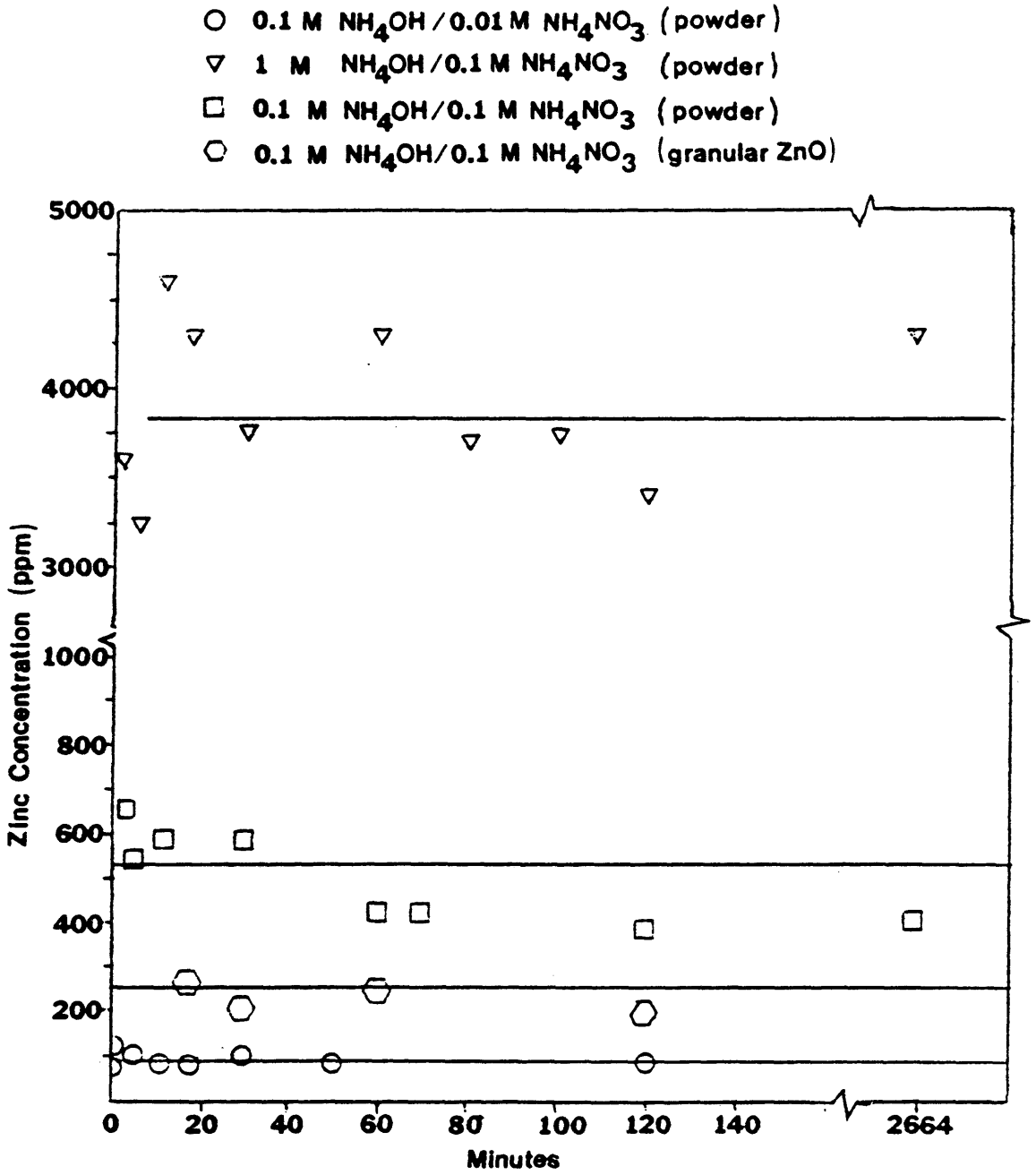

Figure 13

Zinc Concentration Versus Time

Ammonia Lixiviants

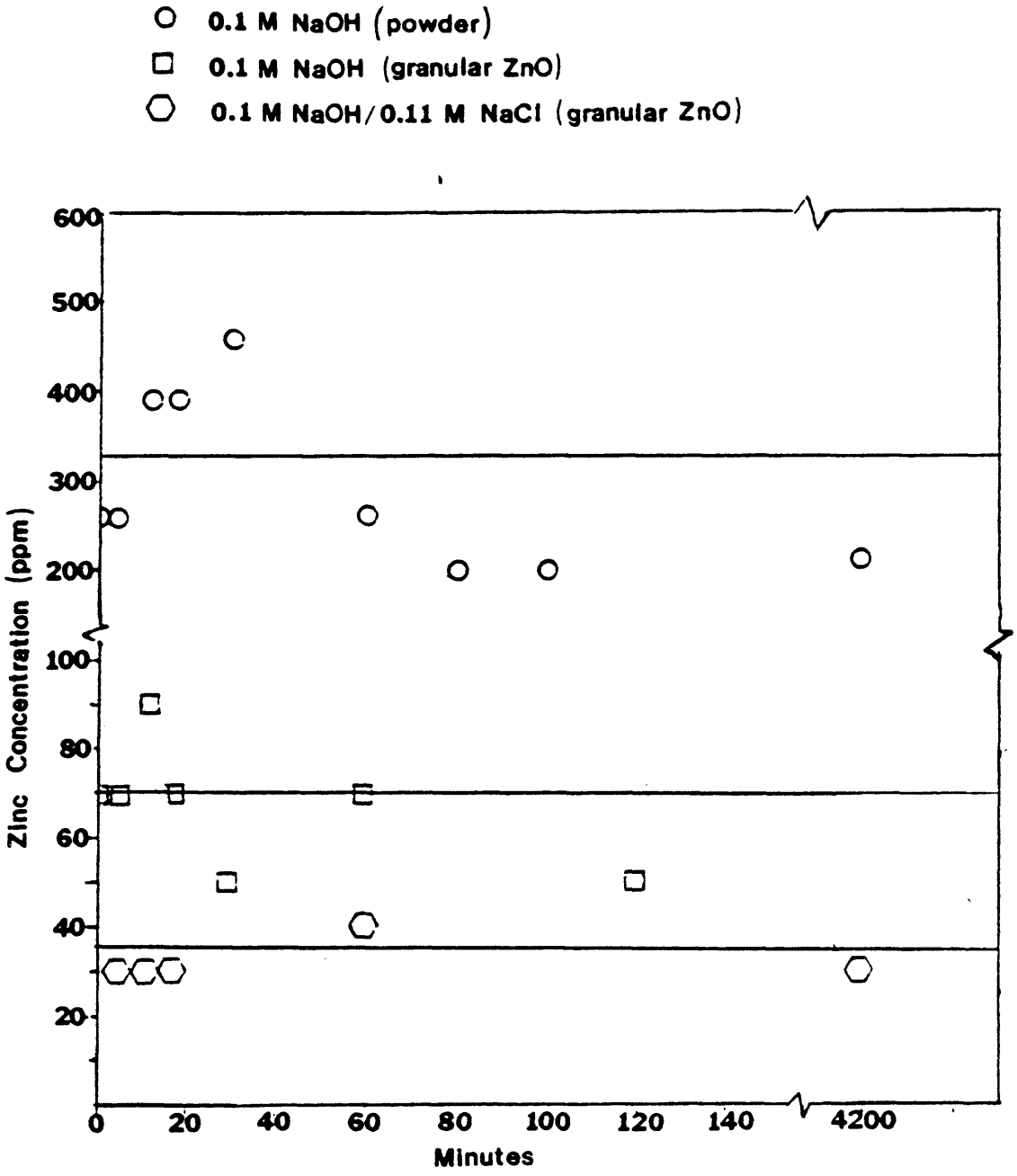

Figure 14

Plot of Zinc Concentration Versus Time
Sodium Hydroxide Lixiviants

Table 2

Summary of Bottle Test Results

Leachant	Equilibrium Concentration (ppm)	Data in figure
0.1 M NH_4OH 0.01 M NH_4NO_3	80	12
0.1 M NH_4OH 0.1 M NH_4NO_3	530	12
0.1 M NH_4OH 0.1 M NH_4NO_3 (granular ZnO)	225	12
1 M NH_4OH 0.1 M NH_4NO_3	3770	12
0.1 M NaOH	310	13
0.1 M NaOH (granular ZnO)	70	13
0.1 M NaOH (granular ZnO) 0.11 M NaCl	34	13

Zinc samples were powdered unless noted granular

Column Experiments

Plots were made of zinc concentration and pH of the column effluent as a function of pore volumes of solution injected. A pore volume (PV) is defined as the volume of solution required to pass through the column bed one time. Table 3 summarizes experimental runs for the two columns used in this research. Figures 15 through 22 deal with the 0.15 M ammonium hydroxide / 0.005 M ammonium nitrate system. Figures 23 through 25 are for the 0.25 M ammonium hydroxide system while figures 26 through 28 deal with the 0.01 M sodium hydroxide / ammonium nitrate systems.

In addition, the total ammonia as determined by ion chromatography for one run for each system is shown in Figures 29 through 31. It should be noted that the drawn curves on all plots have no theoretical basis; they are included to help the reader follow the trends.

Table 3

Column Run Summary
Given in the Sequence which Lixiviants
were Introduced to Each Column

Run No.	Column No.	NH_4OH (M)	NH_4NO_3 (M)	NaOH (M)	Flowrate mL/min	Figure
1	1	0.15	0.005	-	1.62	15
2	1	0.15	0.005	-	1.62	16
3	1	-	0.005	0.01	1.65	26
4	1	0.25	-	-	1.62	25
5	1	0.25	-	-	3.13	24
6	1	0.25	-	-	6.21	23,31
7	1	0.15	0.005	-	1.58	17
8	1	0.15	0.005	-	6.29	18
9	1	0.15	0.005	-	1.60	19
1	2	0.15	0.005	-	1.61	20
2	2	0.15	0.005	-	1.57	21
3	2	0.15	0.005	-	1.62	22,29
4	2	-	0.005	0.01	1.60	27
5	2	-	0.008	0.01	1.62	28

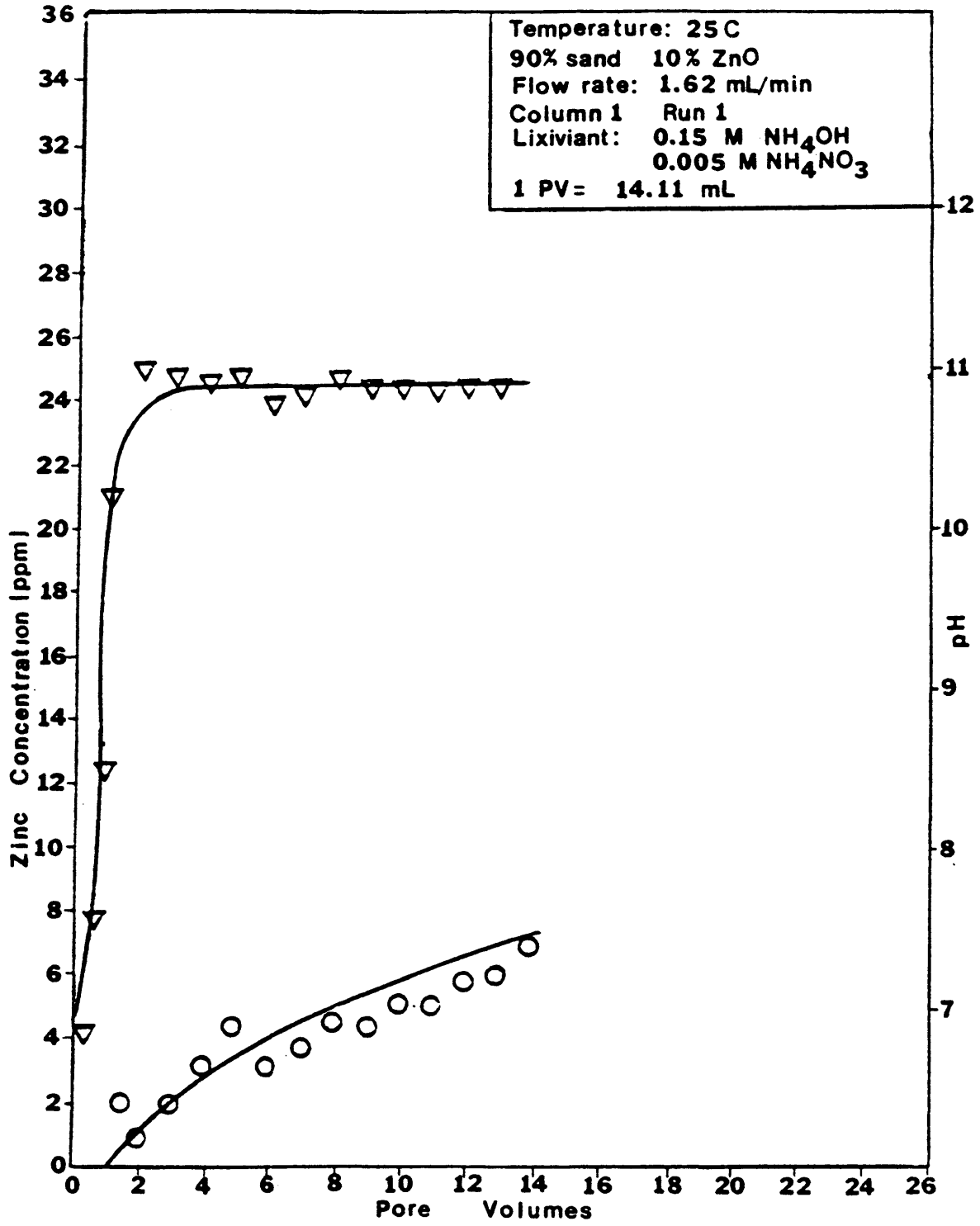

Figure 15

Zinc Concentration and pH Versus Pore Volume
(▽ = pH ○ = Zinc Concentration)

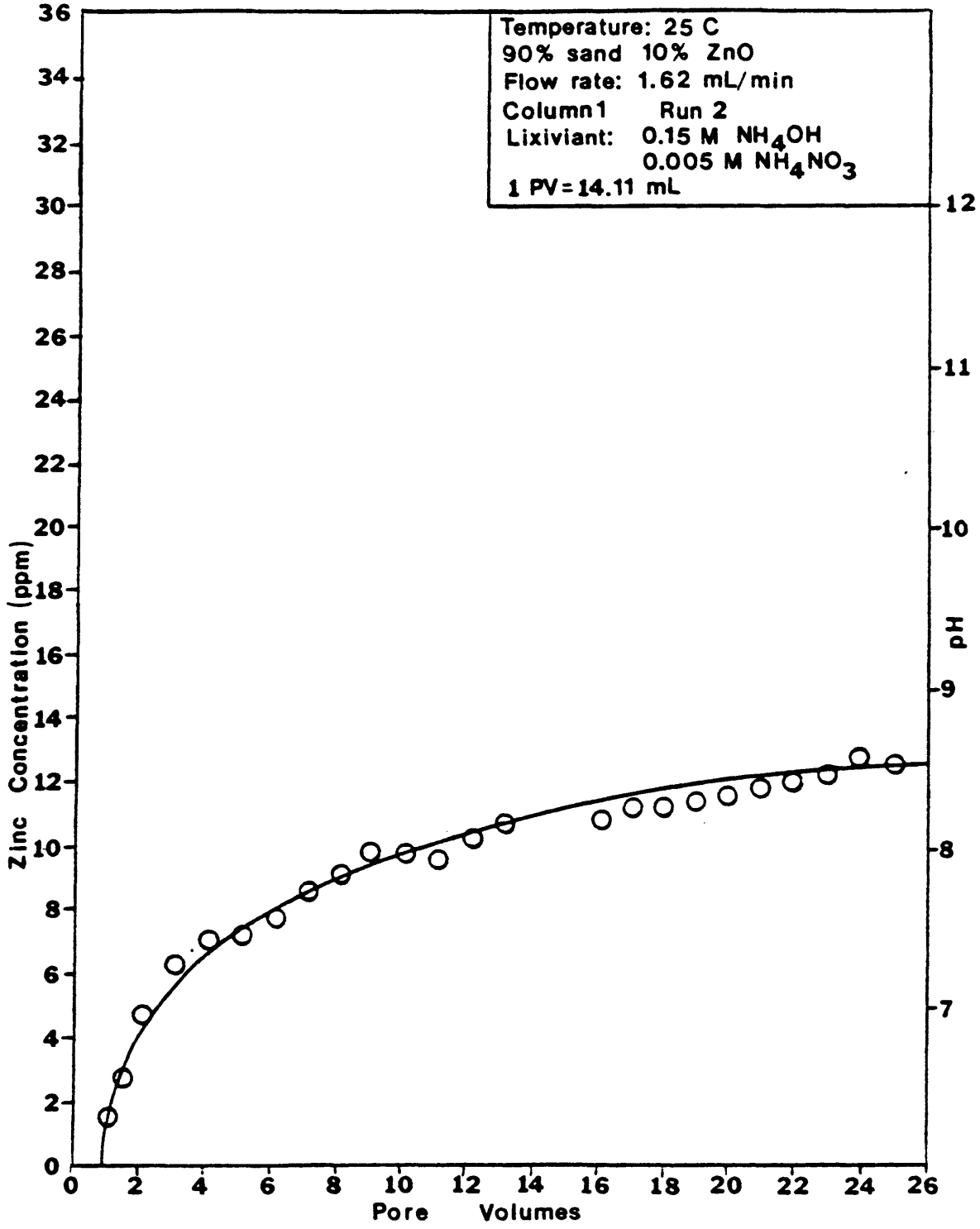

Figure 16
Zinc Concentration Versus Pore Volume
(O = Zinc Concentration)

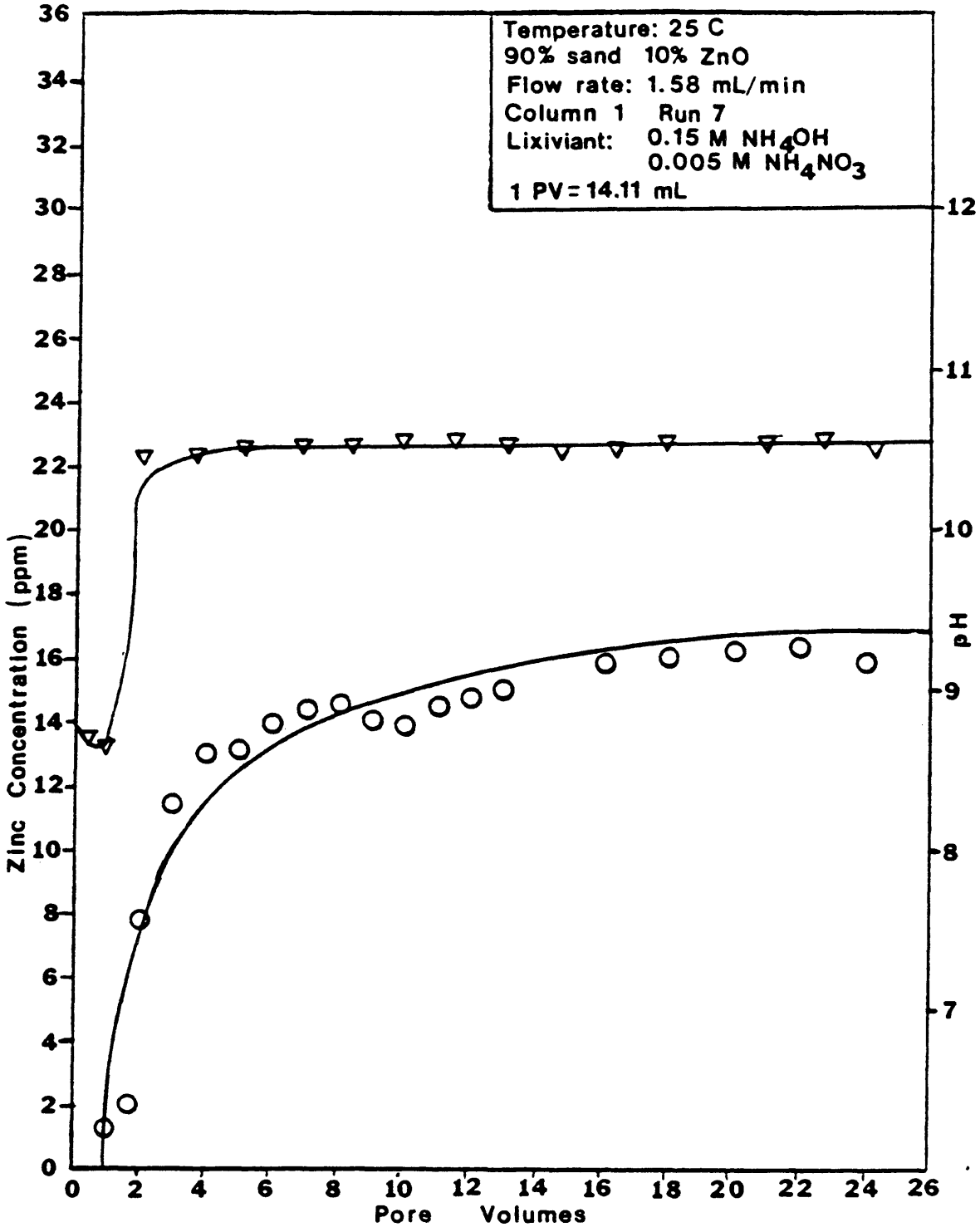

Figure 17

Zinc Concentration and pH Versus Pore Volume
(▽ = pH ○ = Zinc Concentration)

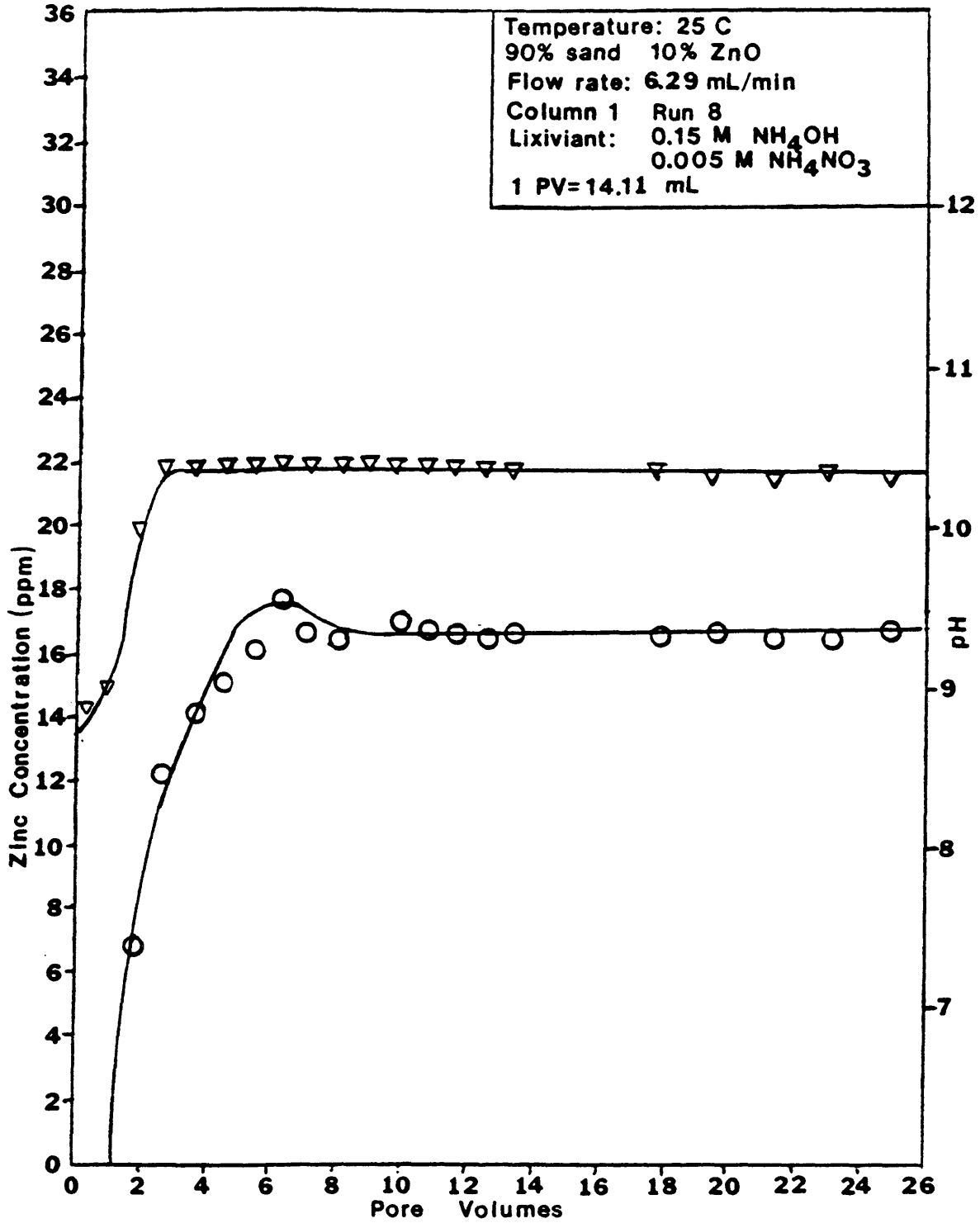

Figure. 18

Zinc Concentration and pH Versus Pore Volume
(▽=pH O= Zinc Concentration)

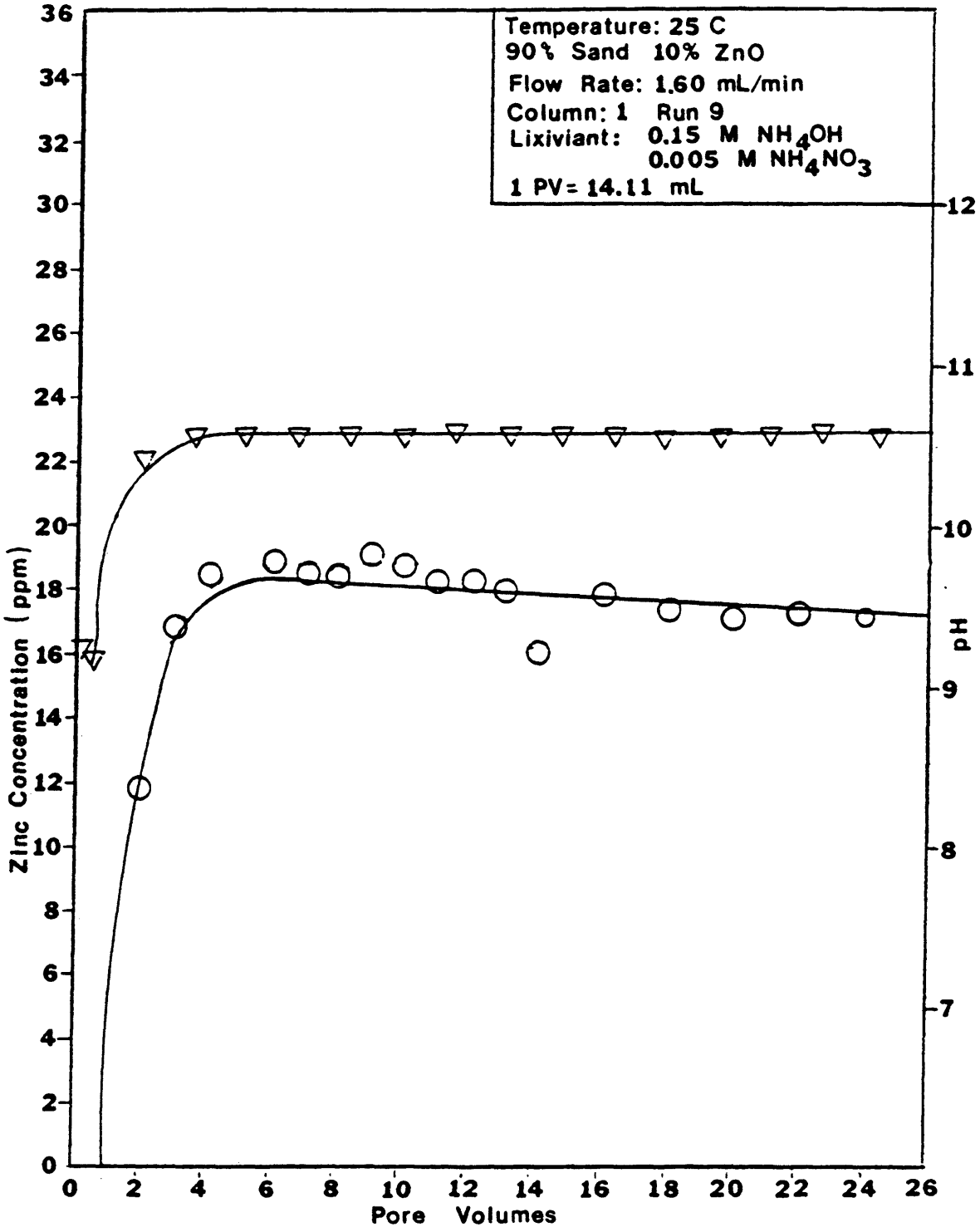

Figure 19

Zinc Concentration and pH Versus Pore Volume
(▽= pH O= Zinc Concentration)

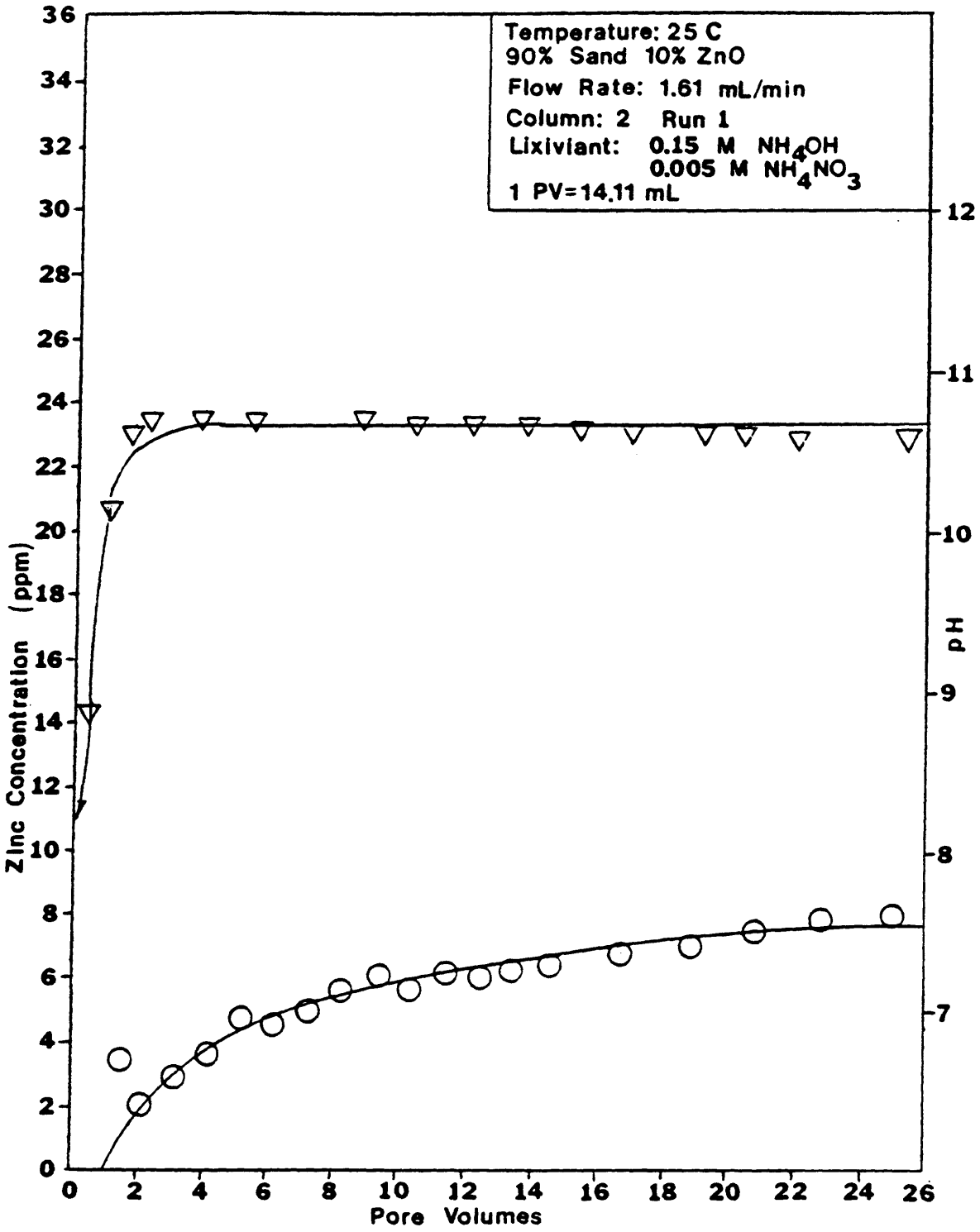

Figure 20

Zinc Concentration and pH Versus Pore Volume
(▽= pH ○= Zinc Concentration)

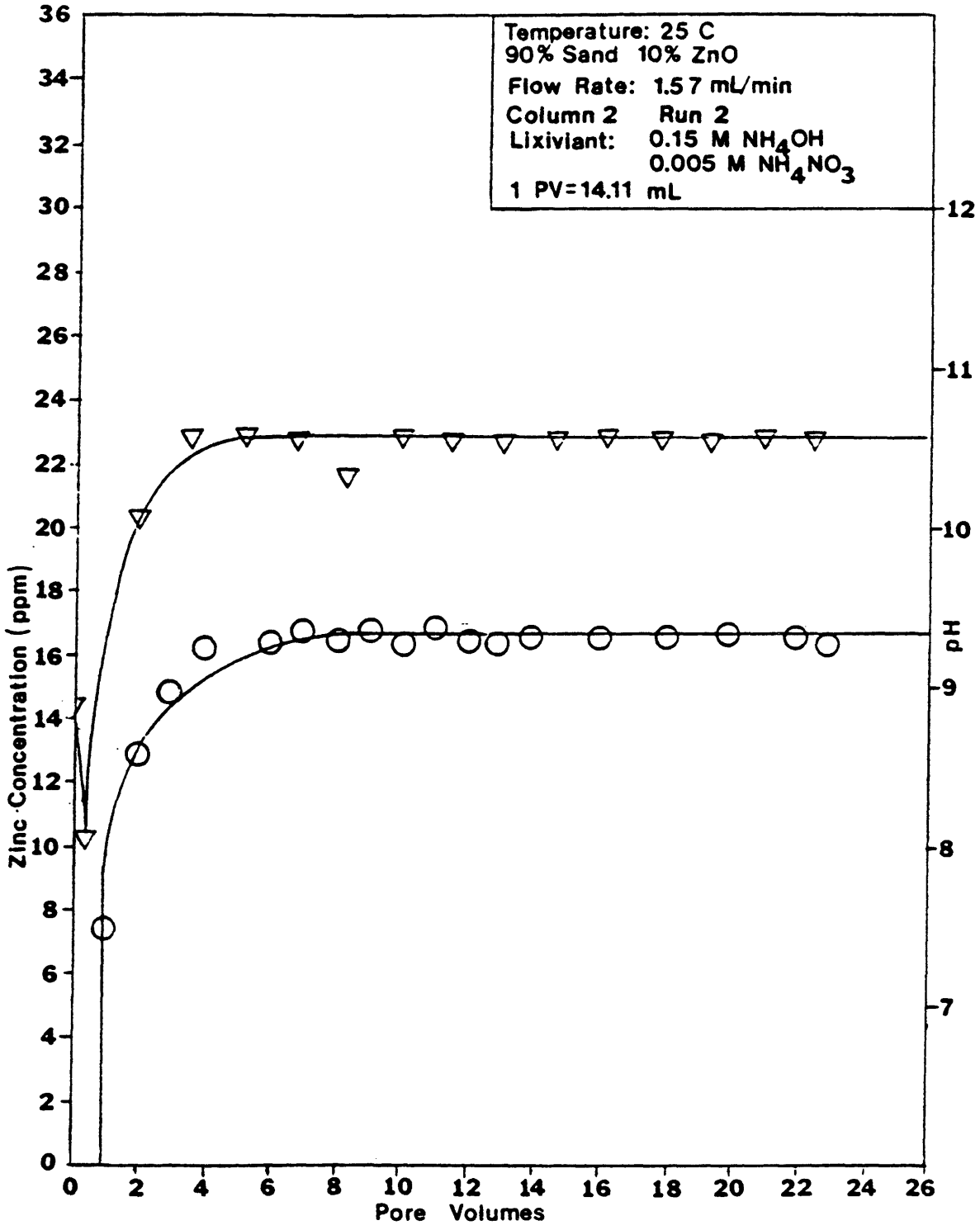

Figure 21

Zinc Concentration and pH Versus Pore Volume
(▽ = pH ○ = Zinc Concentration)

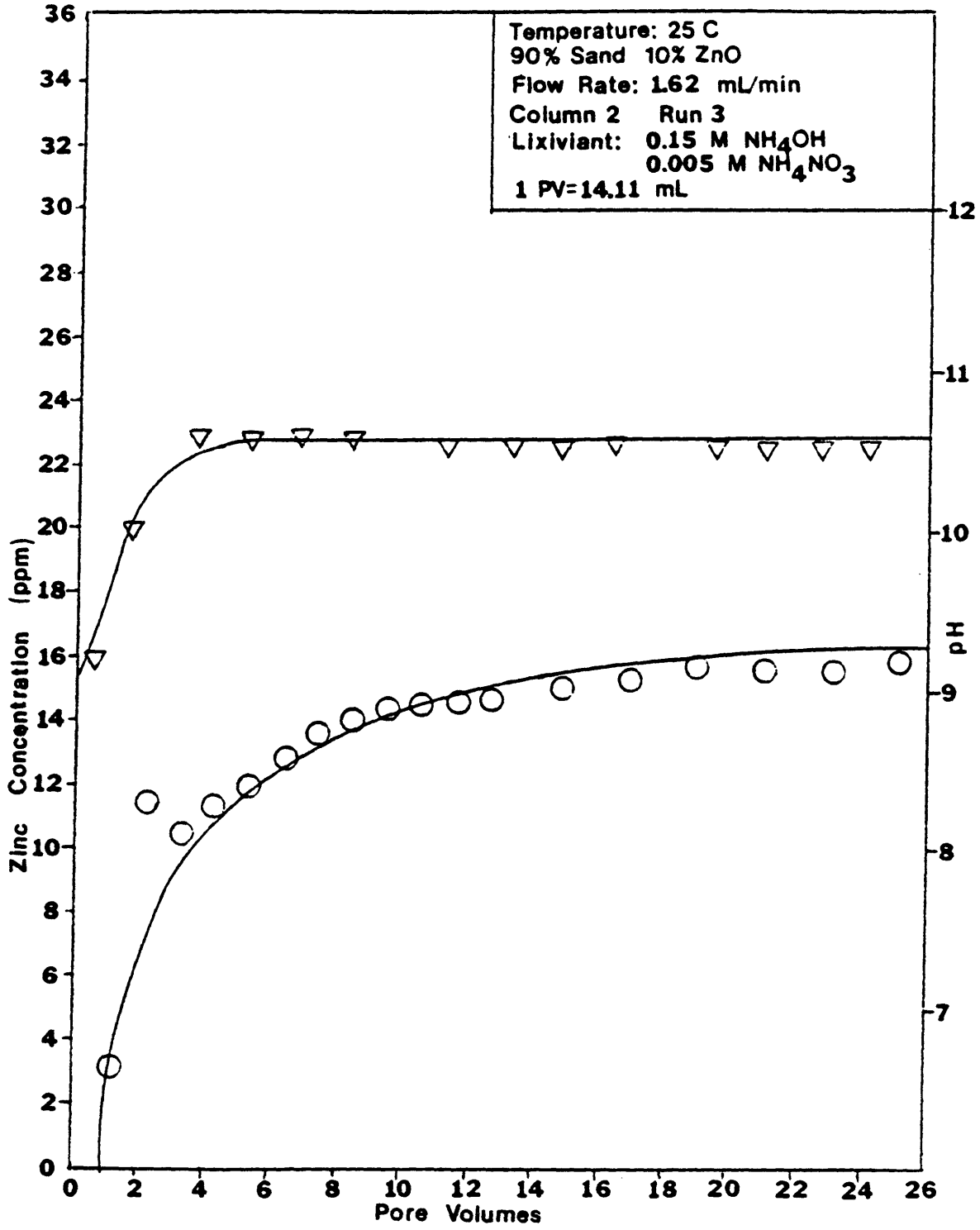

Figure 22

Zinc Concentration and pH Versus Pore Volume
(▽= pH ○= Zinc Concentration)

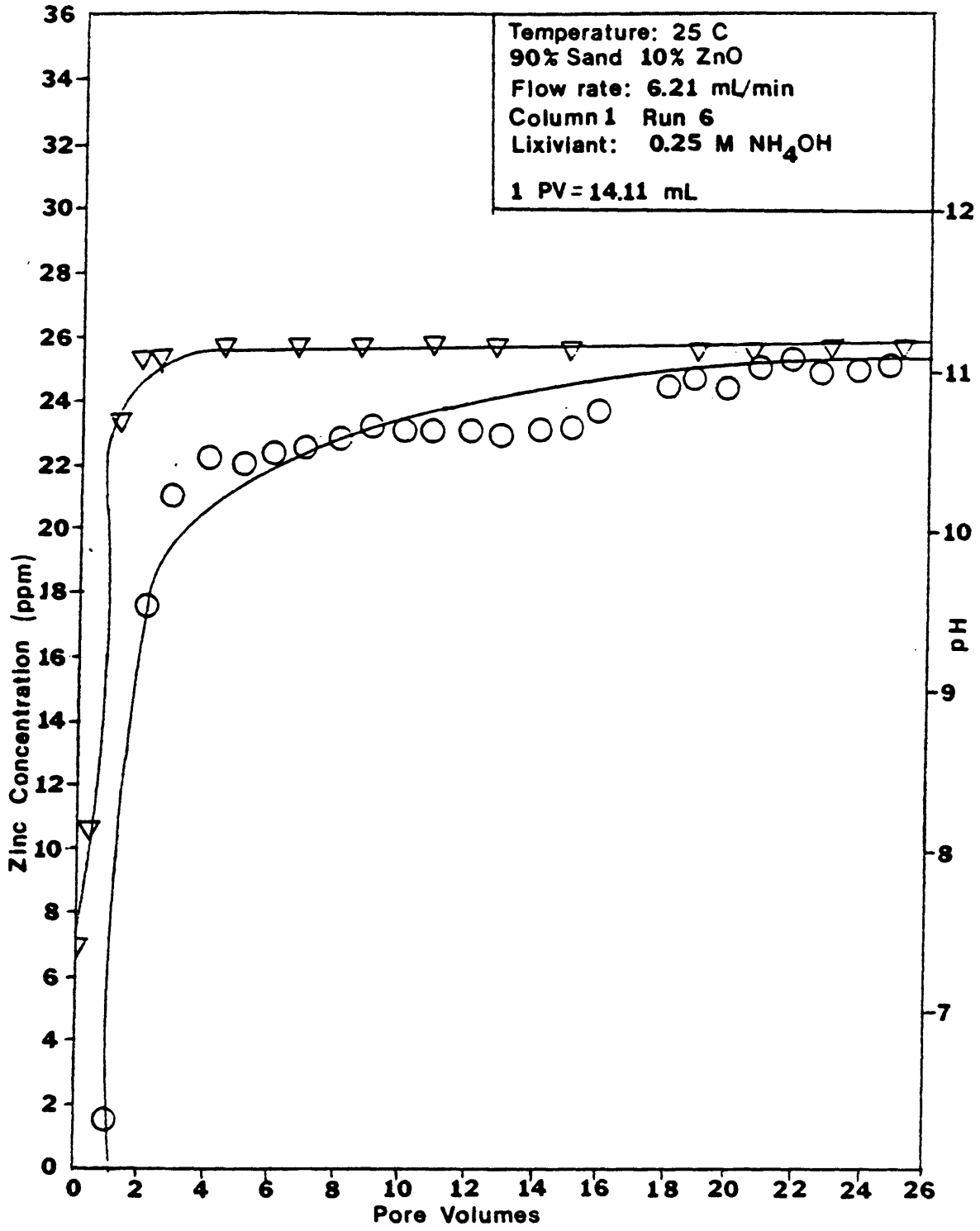

Figure 23

Zinc Concentration and pH Versus Pore Volume
(▽ = pH ○ = Zinc Concentration)

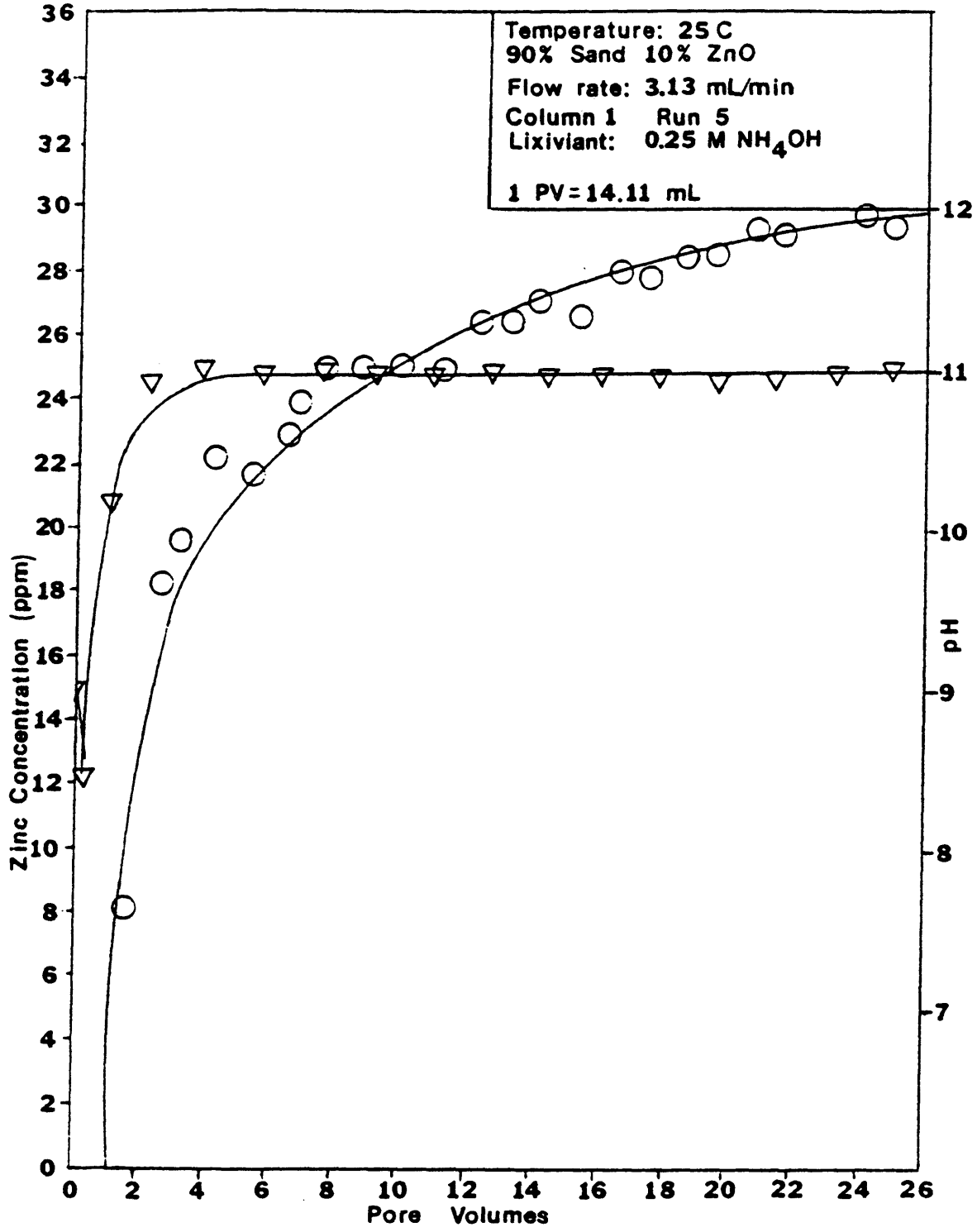

Figure 24

Zinc Concentration and pH Versus Pore Volume
(▽ = pH ○ = Zinc Concentration)

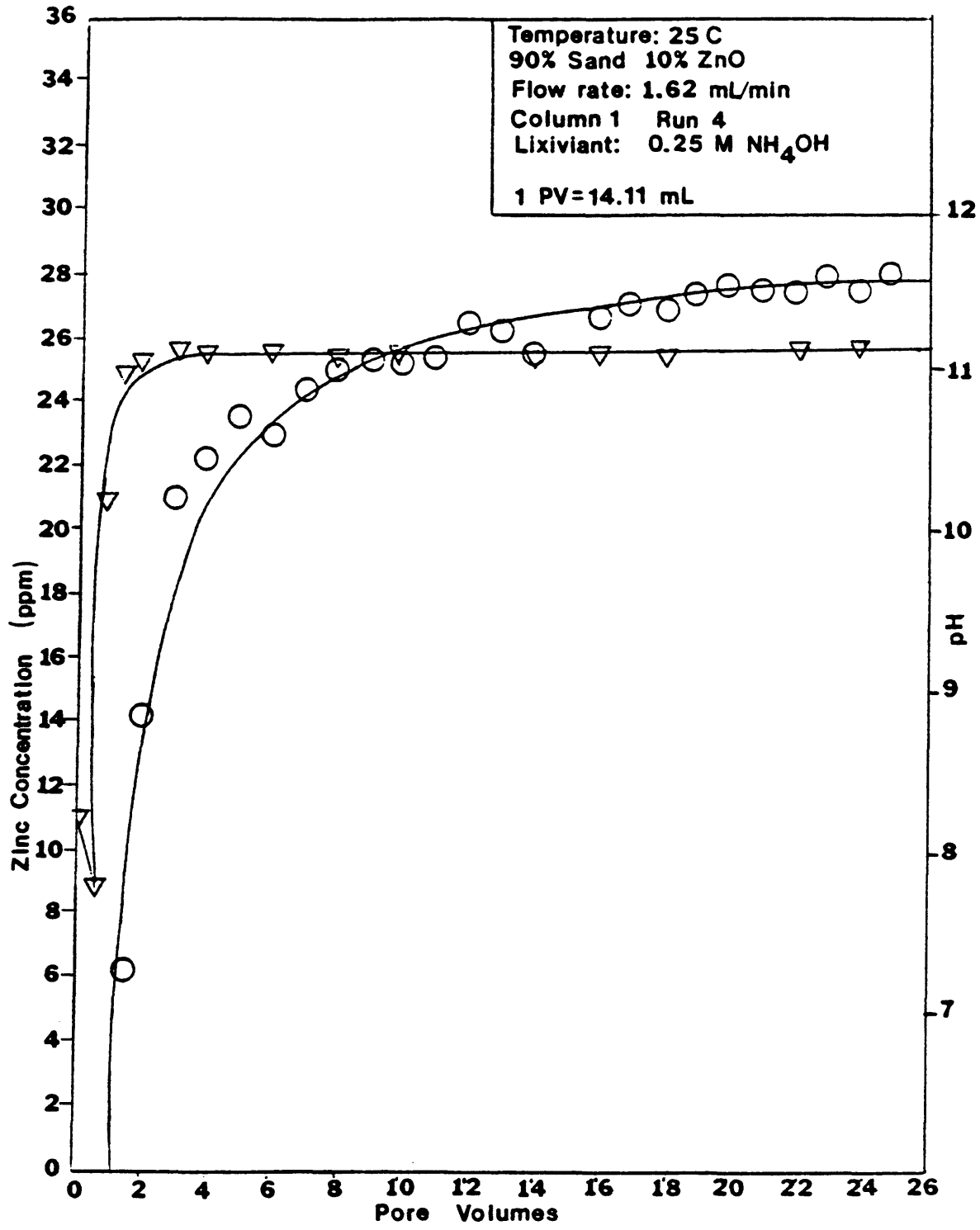

Figure 25

Zinc Concentration and pH Versus Pore Volume
(▽ - pH ○ = Zinc Concentration)

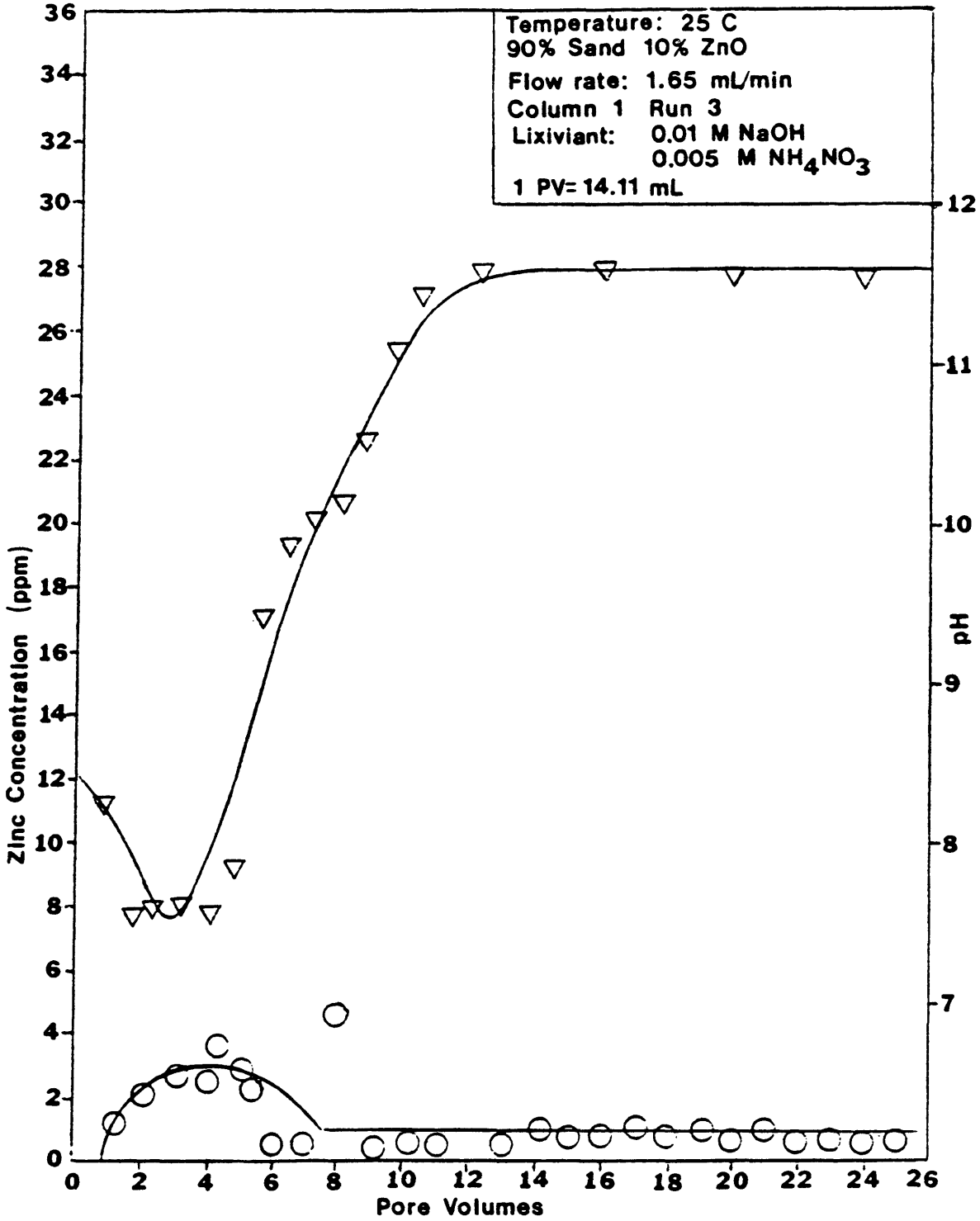

Figure 26

Zinc Concentration and pH Versus Pore Volume
(▽=pH ○=Zinc Concentration)

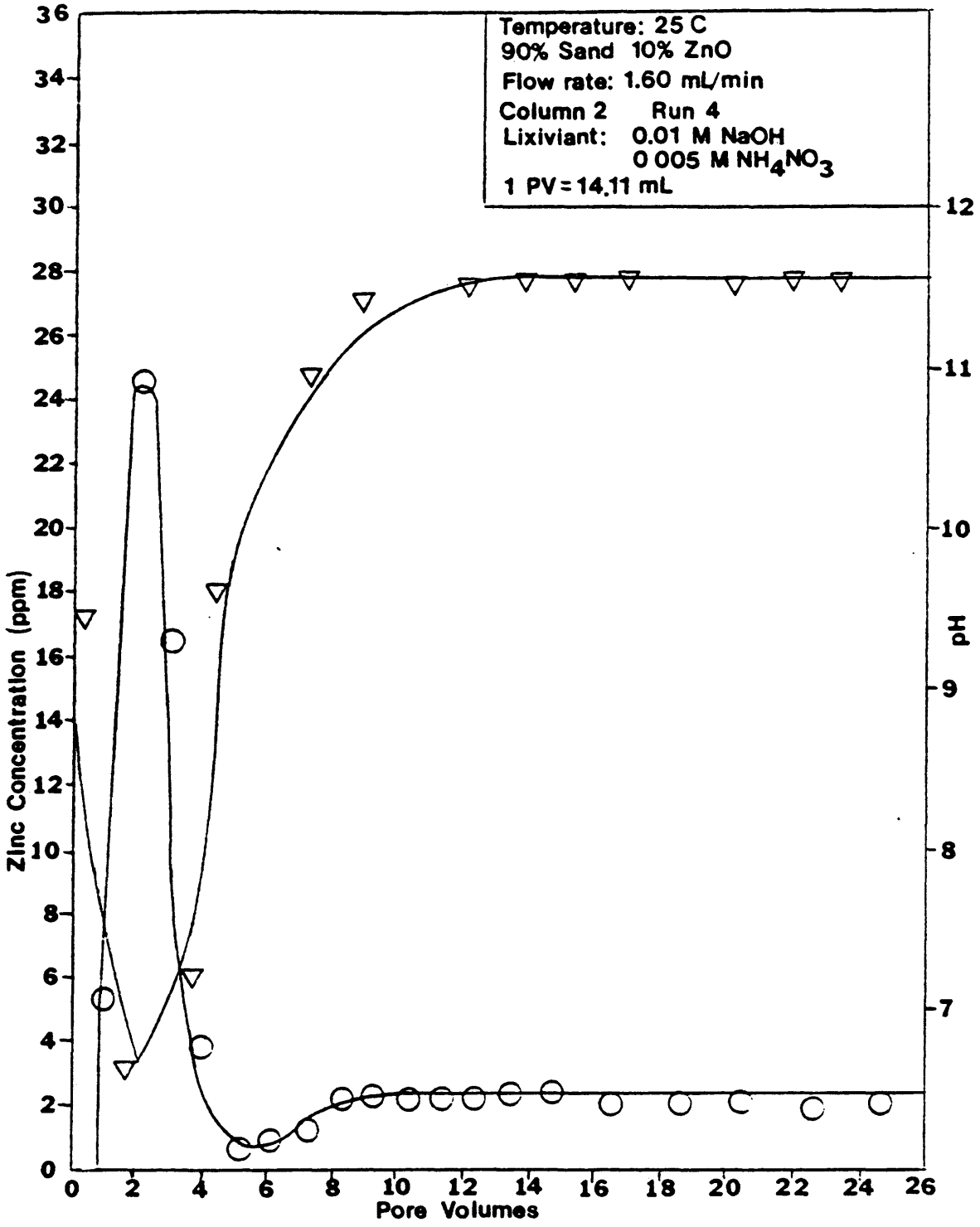

Figure 27

Zinc Concentration and pH Versus Pore Volume
(▽=pH ○= Zinc Concentration)

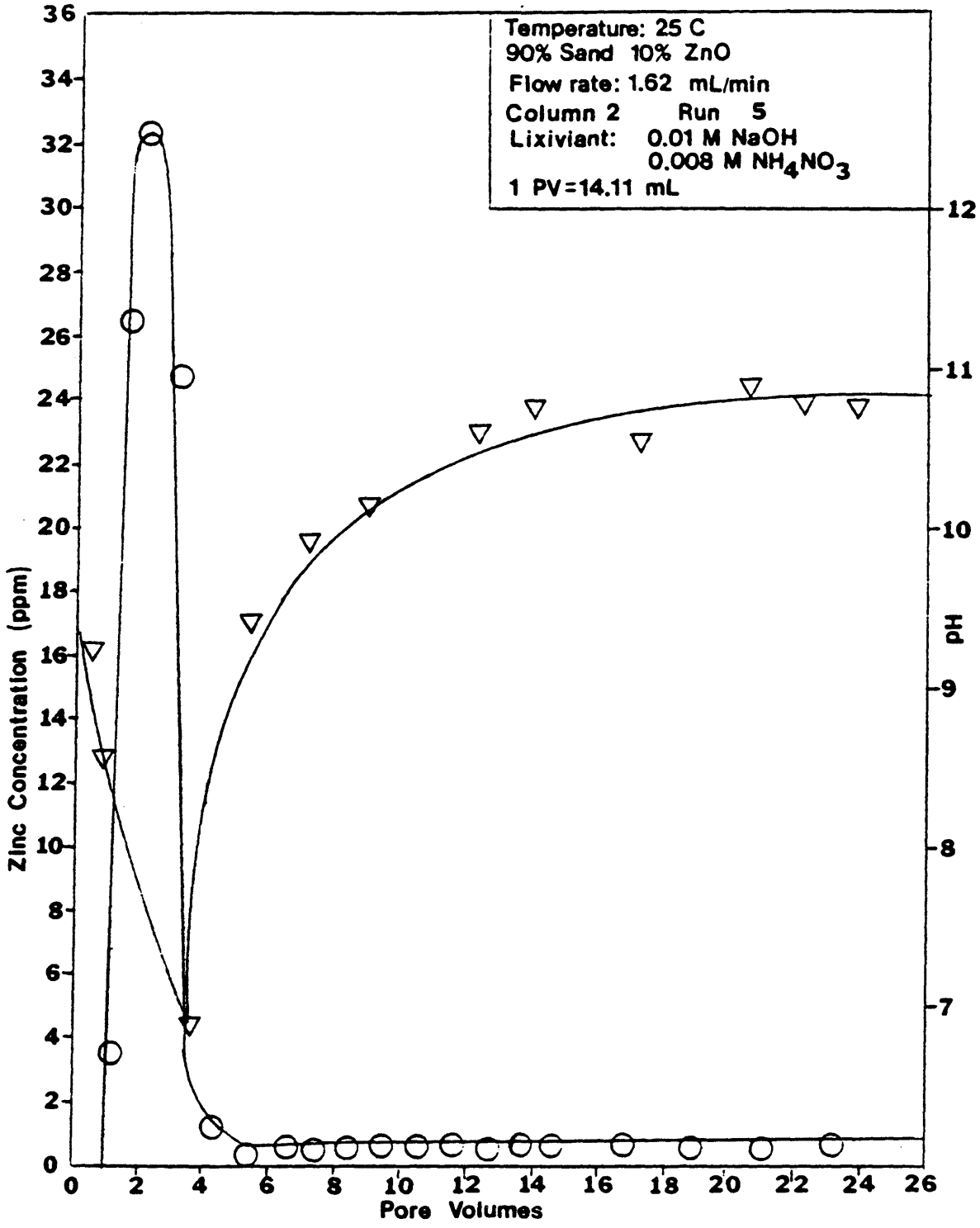

Figure 28

Zinc Concentration and pH Versus Pore Volume
(▽=pH ○= Zinc Concentration)

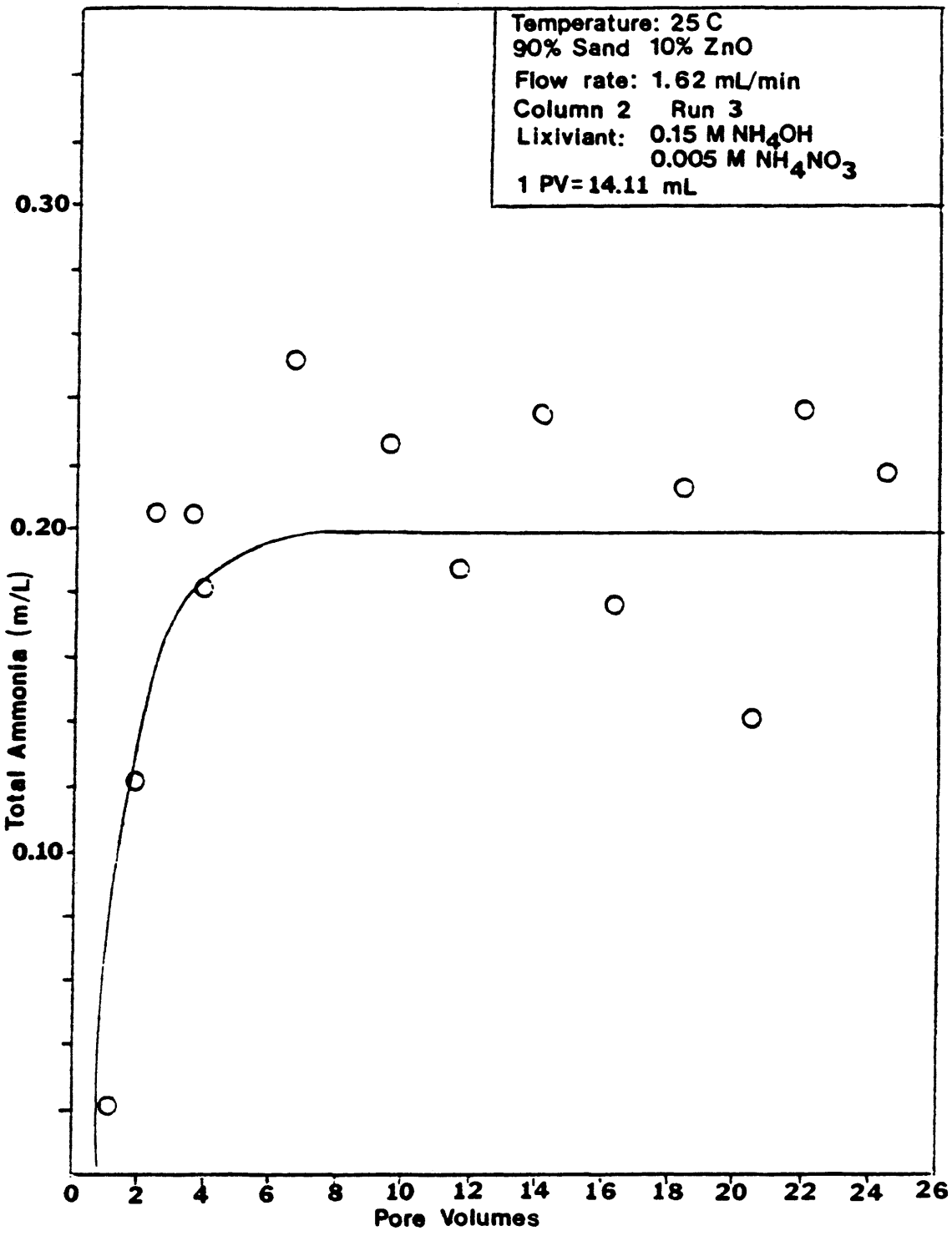

Figure 29
Total Ammonia Versus Pore Volume

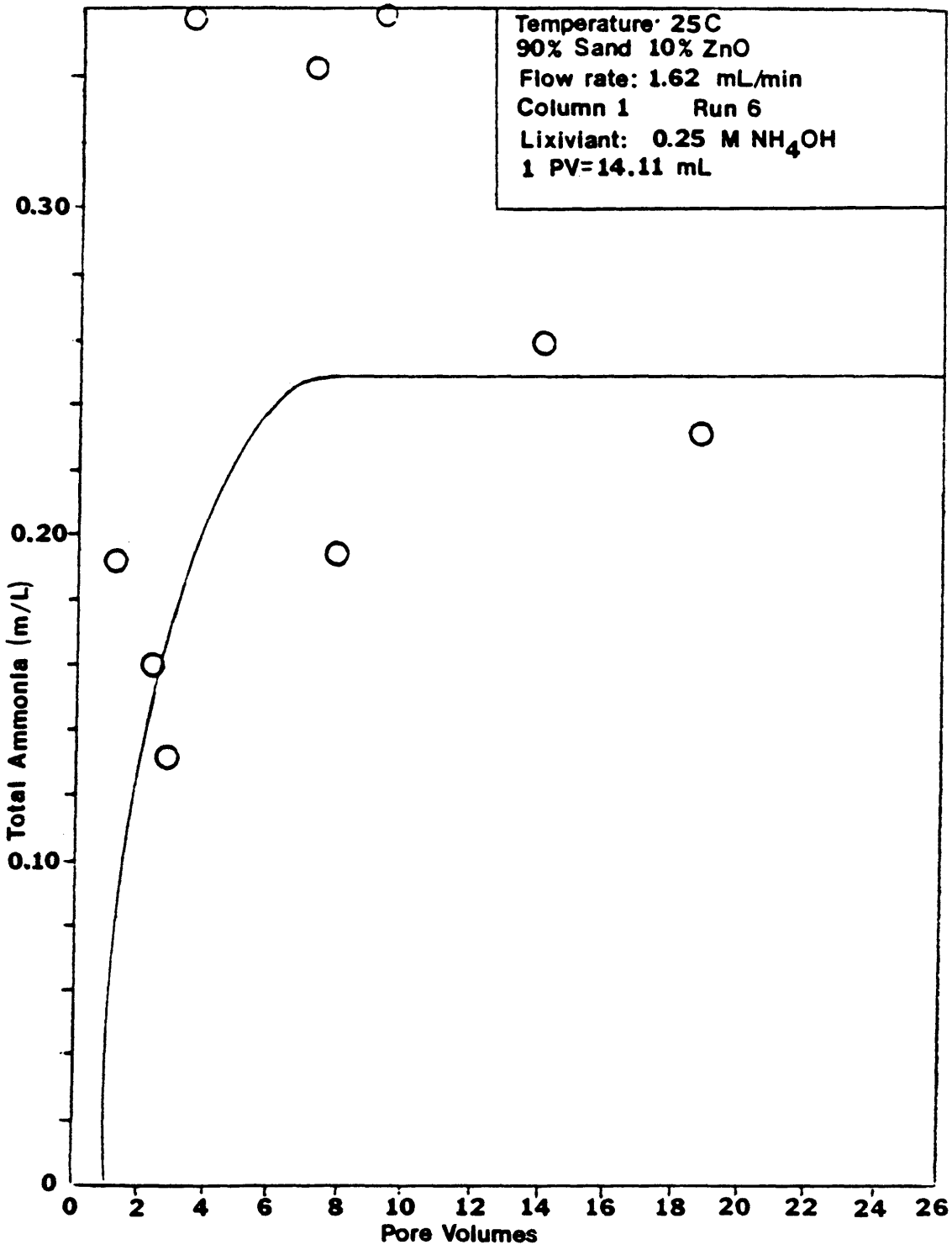

Figure 31

Total Ammonia Versus Pore Volume

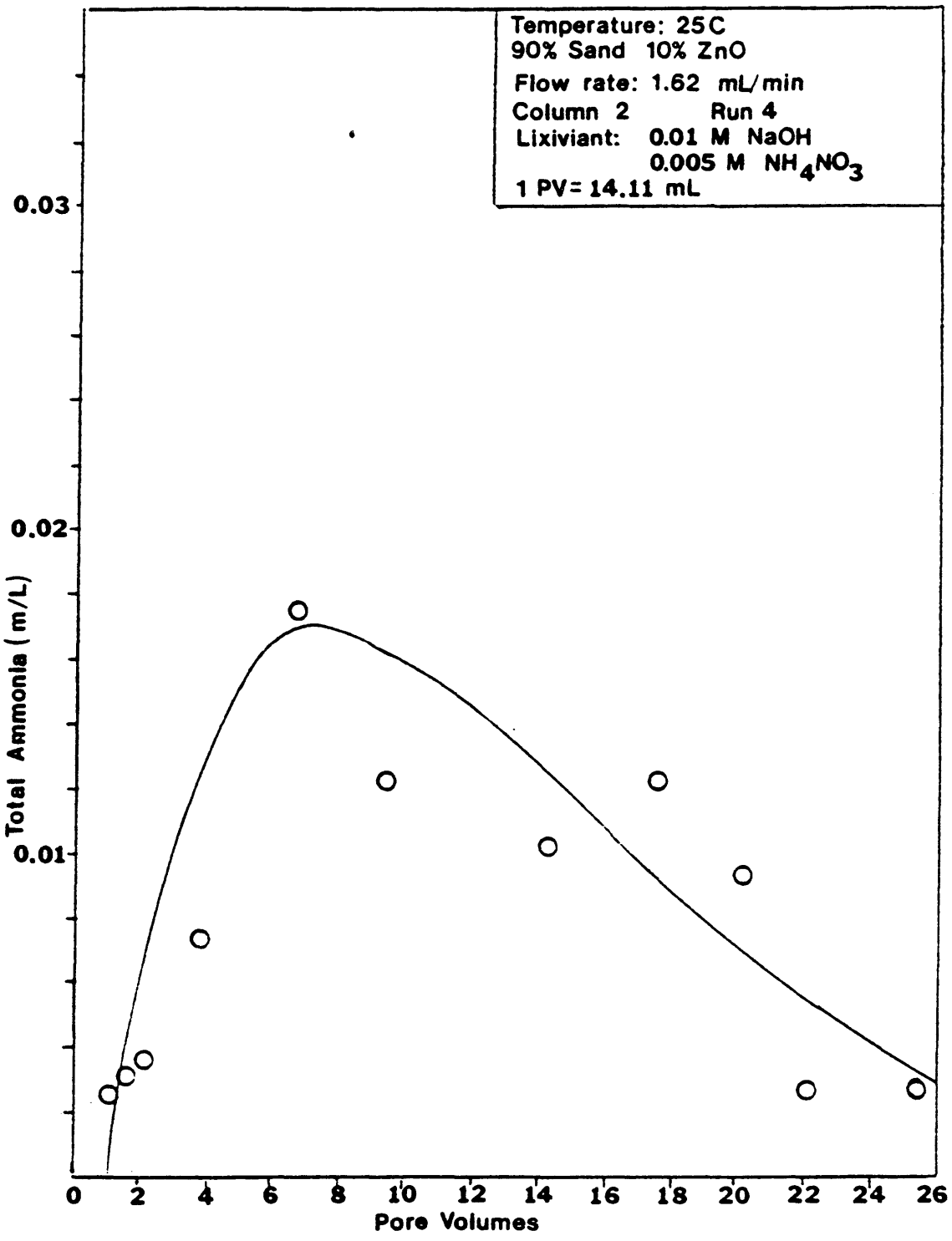

Figure 30

Total Ammonia Versus Pore Volume

Chapter 5
DISCUSSION OF RESULTS

Bottle Experiments

The bottle tests indicate the ammonium hydroxide / zinc oxide leaching system has fast kinetics. The zinc concentration in the lixiviant rapidly comes to an equilibrium plateau. The higher the ammonium ion concentration, the higher the zinc equilibrium plateau.

However, increasing pH level with sodium hydroxide does not significantly increase the zinc concentration. In the bottle tests, both granular and powdered zinc oxide were studied. The powdered zinc oxide resulted in a higher plateau than that of the granular form. The exact mechanism which caused this result is not understood. For the column tests, the granular form was selected because the powder form would tend to physically migrate in the column in the direction of lixiviant flow.

Column Experiments

First of all, it should be noted that multiple runs were performed on a single column. This practice is

justified by the low zinc concentration. Therefore, the amount of zinc removed in comparison to the total zinc oxide particles in the column is negligible. For example, the greatest amount of zinc removal is experienced during runs made using 0.25 M ammonium hydroxide. As illustrated in Figures 23 through 25, this solution has the highest zinc effluent concentration over the longest period of time. For the 0.25 M ammonium hydroxide runs, assuming an average concentration of 25 ppm zinc over 25 PV, the amount of zinc removed is roughly 8 milligrams. When compared to the total amount of zinc oxide in the column, this corresponds to about 0.1% removal per run. In the case of column one, 10 leaching runs were performed giving a total zinc removal of one percent over the life of the column. Only 5 leaching runs were performed on column two.

The chromatography of the leaching solution through the column is influenced by weak acid groups which exist on the surface of minerals. A site on a mineral oxide surface, MOH, can weakly dissociate according to:

$$MOH = MO^- + H^+ \quad (1)$$

and consequentally be neutralized by cations which might be present such as sodium or ammonium with a net result:

$$MOH + Na^+ = MONa + H^+ \quad (2)$$

$$MOH + NH_4^+ = MONH_3 + H^+ \quad (3)$$

Any hydrogen ions produced in these cation exchange reactions must additionally satisfy the equilibrium for dissocation of water and ammonium hydroxide:

$$H_2O = H^+ + OH^- \quad (4)$$

$$NH_4OH = NH_4^+ + OH^- \quad (5)$$

If undissociated ammonium hydroxide is present, removal of the ammonium ions by cation exchange with the mineral surface generates hydroxide ions (Equation 5) to neutralize hydrogen ions released in the exchange (Equation 3).

The pH response observed during the column runs depended on the concentration of the undissociated ammonium hydroxide of the leaching solution. When the ammonium hydroxide concentration is low, hydrogen exchange by Equation (2) combined with Equation (4) appears as a consumption of hydroxide ions and is chromatographically indicated by the delayed pH responses seen in Figures 26, 27, and 28. However, when the ammonium hydroxide concentration in the leaching solution exceeds the capacity of the mineral surface area to react, then Equations (4) and (5) tend to maintain the response pH near the injected value with only a very minimal delay. This chromatographic response is shown in Figures 15 through 25.

These different pH responses provoked correspondingly different responses in the zinc effluent concentrations.

In the case of the ammonium hydroxide / ammonium nitrate lixiviants, the zinc concentration climbs slowly eventually reaching a plateau value. This is shown in Figures 15 through 25. In contrast, the sodium hydroxide / ammonium nitrate lixiviants exhibited peaks in the zinc concentration which exceeded the equilibrium concentration value of the injected leaching solution. The zinc concentrations declined to lower levels when the pH began to increase. This is shown in Figures 26 through 28.

The peak zinc concentration on column 1 is less pronounced than that observed from column 2, although correspondence between pH and zinc concentration is indicated. When the ammonium salt concentration is increased from 0.005 M to 0.008 M the peak zinc concentration increases. In addition, the final pH of the 0.008 M ammonium nitrate solution is lower than the 0.005 M solution because the ammonium hydroxide equilibria (Equation 5) shifts toward the neutral species.

The bottle tests for zinc solubility indicate a strong dependence on the concentration of ammonium ions. Apparently, when the higher pH solutions depress the ammonium ion concentration in the column experiments zinc solubilization is also depressed.

The response in total ammonia show some interesting

results. The ammonia concentrations observed with the 0.01 M sodium hydroxide / 0.005 M ammonium nitrate (Figures 27 and 30) lixiviant does correspond with the pH response. The peak in zinc concentration and minimum in pH are associated with the maximum in total ammonia. There is considerable scatter in the data. Part of this may have been due to inadequate temperature control of the conductivity cell. The cell was insulated but immersion in a constant temperature bath would have been preferable. This was not possible with this unit.

The ammonia effluent response from experiments with the 0.25 ammonium hydroxide (Figures 23 and 31) and the 0.15 M ammonium hydroxide / 0.005 M ammonium nitrate (Figures 22 and 29) lixiviants are more perplexing. Again, there is considerable data scatter which complicates interpretation. In addition, the data in Figure 29 appear to plateau at a total ammonium concentration of 0.2 M which is larger than the actual total of 0.155 M. This suggests a systematic error perhaps in the calibration or sample dilution in addition to the conductivity cell temperature control problem. Despite these complications, Figure 29 indicates that the concentration of total ammonia increases steadily with throughput. By contrast, Figure 31 suggests a peak in total ammonia before settling to a plateau concentration of

about 0.25 M. The cause of this is not clear, although it may be connected with the pH dependence of the ion exchange equilibria of the solid surface and the ammonia speciation.

When ammonium hydroxide concentrations are large, as in the case of the 0.25 M ammonium hydroxide and 0.15 M ammonium hydroxide / 0.005 M ammonium nitrate leaching solutions, the effluent zinc concentrations approach the plateau values shown in Table 4.

Early runs on both columns 1 and 2 indicate a conditioning phenomena. For example, in run 1 on column 1 (Figure 15) the apparent plateau level was 8 ppm zinc. In subsequent runs with same lixiviant and flow rates (Runs 1 and 7) the plateau value increased to 12 ppm zinc and 16 ppm zinc. Run number 9 has nearly the same effluent zinc concentration as run number 7 suggesting that the column had stabilized. This was repeated on column 2 as shown in Figures 20 through 22. In all cases, the plateau values reached in the column experiments fall short of the equilibrium values for similiar lixiviants shown in Figures 13 and 14. The chromatographic phenomena observed in these experiments should be predictable with sufficiently descriptive models. Two models are described here. The first model addresses the gradual increase in zinc concentration to a plateau value and the effect of flow rate on this

Table 4

Values of Zinc Concentration at Plateau
for Various Lixiviants

Lixiviant Composition	Observed Maximum Effluent Zinc Concentration Plateau (ppm)	Figure	Flow Rate (mL/min)
0.15 M NH_4OH 0.005 M NH_4NO_3	16	17	1.58
0.25 M NH_4OH	26	23	6.21
0.01 M NaOH 0.005 M NH_4NO_3	2	27	1.60
0.01 M NaOH 0.005 M NH_4NO_3	1	28	1.62

plateau concentration. The second development outlines the approach needed to explain the ammonia-pH and zinc trends of the sodium hydroxide / ammonium nitrate lixiviant types.

Chromatographic Models

Ammonium Hydroxide / Ammonium Nitrate Solutions

In the case of the ammonium hydroxide / ammonium nitrate solutions, the slow rise in the zinc concentration is hypothesized to be the result of surface adsorption of the various zinc species. Neglecting the axial dispersion, the differential material balance for convective transport of a solute generated by reaction (in this case zinc by dissolution) is given by:

$$\frac{\partial C}{\partial t} + \frac{(1-\epsilon)}{\epsilon} \rho_s \frac{\partial n}{\partial t} + \frac{u}{\epsilon} \frac{\partial C}{\partial z} = r \qquad (6)$$

where C and n are respective concentrations of zinc in solution and adsorbed on the solid, u is the superficial velocity, ϵ is the column porosity, ρ_s is solid density, r is the rate of zinc production, and z and t are axial position and time.

Assuming that solute adsorption is instantaneous, Equation (6) can be rewritten in dimensionless terms for a

column of length L :

$$\frac{\partial\theta}{\partial\tau}\left(1+\alpha\frac{\partial\Gamma}{\partial\theta}\right)+\frac{\partial\theta}{\partial\xi}=\frac{rL\epsilon}{uK}=\gamma \tag{7}$$

$$\tau=\frac{ut}{L\epsilon}\quad;\quad\xi=\frac{z}{L} \tag{8}$$

$$\alpha=\frac{(1-\epsilon)}{\epsilon}K n_{max}\rho_s\quad;\quad\theta=KC\quad;\quad\Gamma=\frac{n}{n_{max}} \tag{9}$$

where K and n_{max} are the adsorption constants which are defined shortly. The dimensionless group γ, called the Damköhler number, is a measure of the time for reaction compared to the residence time for the reacting solution. As observed in the bottle and column tests, dissolution rates appear to be mass transfer limited. Also, since the zinc concentration in the effluent is very small, the concentration of the lixiviant is essentially unchanged by zinc dissolution and the zinc solution concentration is negligible compared with its solubility limit.

The zinc production rate might be represented reasonably by:

$$r=k_e C_s \tag{10}$$

where k_e is the external mass transfer coefficient and C_s is zinc solubility limit for the injected lixiviant. Although several zinc species may form and dissolve, a

simple Langmuir expression is chosen to represent the zinc sorption:

$$\Gamma = \frac{n}{n_{max}} = \frac{KC}{1+KC} = \frac{\theta}{1+\theta} \qquad (11)$$

Figure 32 shows typical adsorption curves for different values of K when n is assumed to be 12×10^{-12} g zinc per g solid when the concentration is 3×10^{-5} g zinc per g solution. Small values of K exhibit less curvature, while large values approach a step increase.

Before introduction of lixiviant into the column zinc solubility, C, is essentially zero and zinc production will be essentially zero according to Equation (10). However, zinc solubility quickly increases to C_s for the leaching solution introduced into the column.

Equation (7) is now solved using the method of characteristics. This produces two ordinary differential equations which will hold along a characteristic curve.

$$\frac{d\theta}{d\xi} = \gamma \qquad (12)$$

$$\frac{d\tau}{d\xi} = 1 + \frac{a}{(1+\theta)2} \qquad (13)$$

Solving Equation (12) yields the zinc concentration as a function of dimensionless position. The leaching solution will advance through the column with a dimensionless

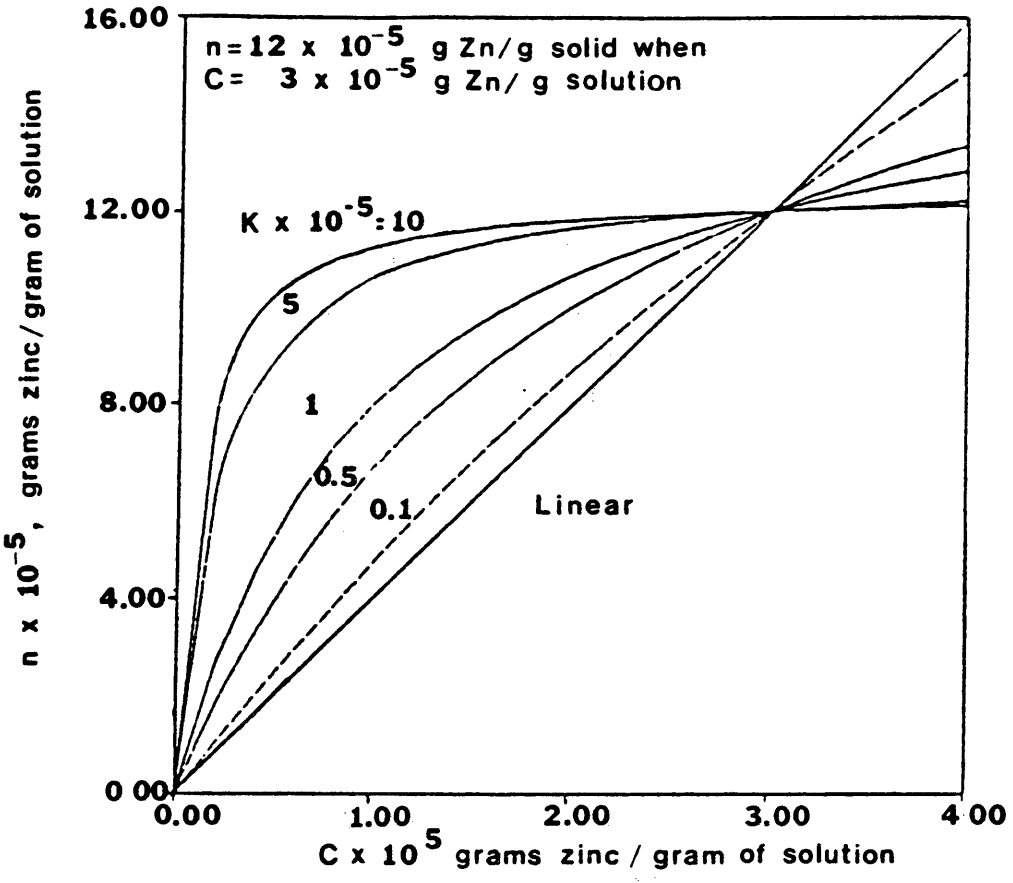

Figure 32 - Adsorption Isotherm for Various Values of K

velocity of one if there is no ion exchange delay of the leaching solution. Assuming that ξ_1 is the position which leaching solution has reached in time τ, Equation (12) gives:

$$\theta = \gamma(\xi - \xi_1) \tag{14}$$

Incorporating Equation (14) into Equation (13) describes the relationship between dimensionless time and dimensionless position which is solved:

$$\int_{\xi_1}^{\tau} d\tau = \int_{\xi_1}^{\xi} \left\{ 1 + \frac{a}{[1 + \gamma(\xi - \xi_1)]^2} \right\} d\xi \tag{15}$$

or

$$\tau = \xi + \frac{a(\xi - \xi_1)}{1 + \gamma(\xi - \xi_1)} \tag{16}$$

Figure 33 shows the position-time diagram for various values of the adsorption constant, K. In this diagram, γ/K is taken as 2.0×10^{-5} grams zinc/gram of solution. Along each characteristic curve the concentration of zinc is increasing according to Equation (14) where ξ_1 is the attach point of the characteristic curve to the indifferent wave. This attach point is the position which the front of the lixiviant solution has reached in given amount of time, τ. Because the dissolved zinc adsorbs, the velocity of the zinc concentration wave is retarded compared to the frontal

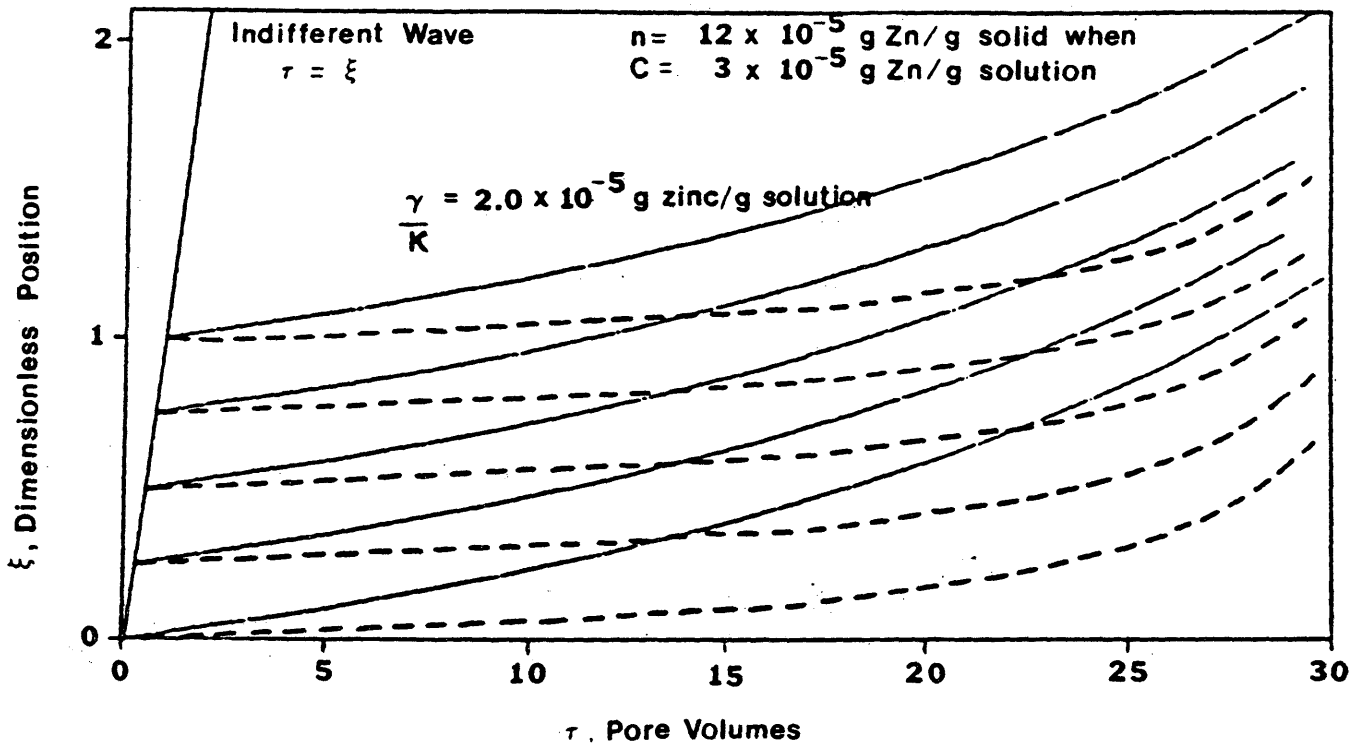

Figure 33 - Characteristic Position Time Diagram for $K = 0.5(10^5)$ g solution/g Zn (solid lines) and $K = 5(10^5)$ g solution/g Zn (dashed lines)

advance rate of the lixiviant.

Three zones develop in the column. Ahead of the lixiviant, the solubility of the zinc is zero. After lixiviant has been injected for along time, the column is filled with lixiviant and the concentration of the dissolved zinc depends only on position and the ratio of dissolution rate to solution residence time. In the intermediate zone, the concentration of zinc increases gradually from zero to the position-controlled value. The following expressions summarize these results:

$$\theta = 0 \qquad \xi \geq \tau \geq 0 \tag{17}$$

$$\theta = \frac{\gamma(\tau-\xi)}{a-\gamma(\tau-\xi)} \qquad \left[\xi - \frac{a/\gamma}{1+\gamma\xi}\right] \geq \tau \geq \xi \tag{18}$$

$$\theta = \gamma\xi \qquad \tau \geq \left[\xi - \frac{a/\gamma}{1+\gamma\xi}\right] \tag{19}$$

The predicted concentration histories are shown in Figure 34 for a dimensionless position of 1 (at the outlet of the column).

According to this diagram, adsorption of the dissolved species (in this case zinc) does make for a gradual increase in the column effluent. If the isotherm is linear, the concentration rises linearly with time. In

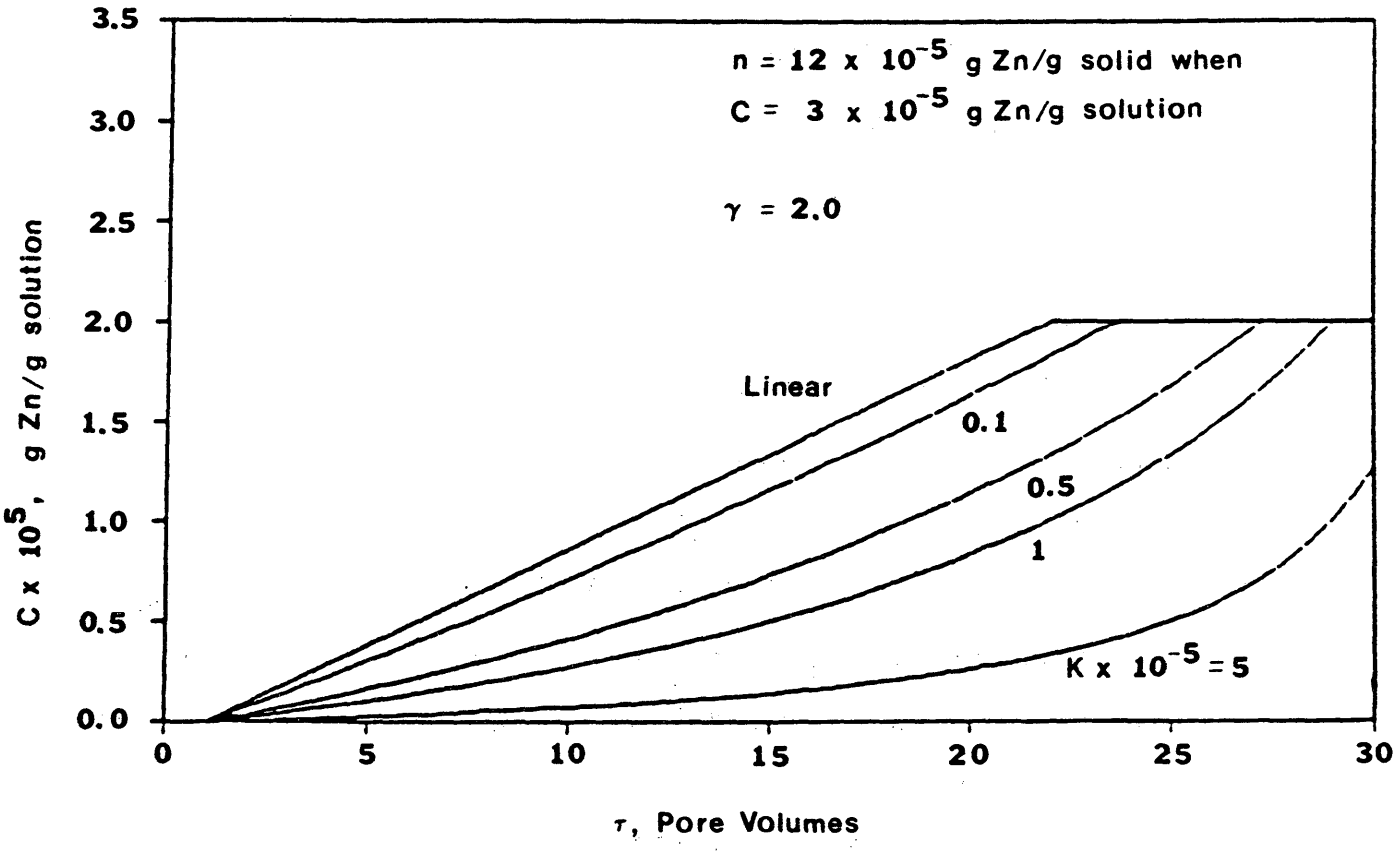

Figure 34 - Concentration History of a Dissolving and Adsorbing Species

this case, the chromatographic theory predicts that the effluent zinc concentration would require nearly 21 pore volumes to increase linearly from zero to the plateau concentration of 2.0×10^{-5} grams zinc/gram solution.

However, in the proposed mechanism, a Langmuir isotherm is suspected. For Langmuir isotherms, increasing K causes the effluent zinc concentration to increase more gradually and to turn concave up which is exactly contrary to observed experimental behavior. The curvature of these theoretical history curves would be revised to concave down, if the proposed adsorption isotherm had been concave up rather than concave down. These results could be independently investigated by measuring zinc adsorption. The quartz gangue material will be principally responsible for adsorption. Adsorption isotherms could be generated by passing zinc laden leaching solutions through columns packed with only quartz and monitoring the concentration of zinc in the effluent. If the isotherm is concave up as hypothesized, a step change increase in zinc would provoke a spread effluent response from which the entire isotherm could be estimated using the technique of Gluekauf, 1949.

The cause of the increase in the plateau value of zinc in repeated runs is not clear. One hypothesis is that the introduction of distilled water into the column after a run

would cause deposition of zinc onto the solid. The zinc deposited in this manner may be more easily dissolved once fresh lixiviant is introduced into the column.

Flow rates effects on the plateau concentration of zinc were not consistent. For example, in the case of the 0.25 M ammonium hydroxide runs (Figures 22, 23, and 24), the plateau value of the zinc concentration did not change consistently with increasing lixiviant flow rate. At a flow rate of 1.6 mL/min, the observed plateau concentration was 28 ppm zinc. At a flow rate of 3.2 mL/min, the plateau was 30 ppm zinc. However, increasing the flow rate to 6.2 mL/min caused the plateau to drop to 26 ppm zinc. In the case of the 0.15 M ammonium hydroxide / ammonium nitrate solutions, very little effect in zinc concentration was noted with varying flow rate.

If the rate of zinc dissolution is independent of the dissolved zinc concentration and flow rate, doubling the residence time by cutting the flow rate in half, should double the concentration of the effluent plateau value. This was not observed.

Since the bottle tests indicate that the solubility limit for zinc in the ammonium hydroxide solutions is much higher than the plateau values observed experimentally, it is not likely that a solubility limit is responsible for a

zinc plateau concentration being effected marginally by the flow rate. The fast rates of dissolution in the bottle tests combined with the limited flow rate dependence in the column experiments indicate external mass transfer limitations. For flow through a packed bed, the mass transfer coefficient, k_e can be calculated by (Sherwood, Pigford and Wilke):

$$k_e = \frac{1.17\,u}{\left[\frac{d_p u}{\nu}\right]^{0.42} Sc^{0.67}} \qquad (20)$$

where u is the fluid velocity, d_p is the average particle diameter, ν is the kinematic viscosity, and Sc is the Schimdt number. The net effect on γ is:

$$\gamma = \frac{k_e C_s L \epsilon}{uK} = \frac{1.17\,C_s L \epsilon / K}{\left[\frac{d_p u}{\nu}\right]^{0.42} Sc^{0.67}} \qquad (21)$$

So decreasing the fluid velocity increases the residence time for dissolution, while simultaneously decreasing the rate of dissolution. These offsetting contributions will tend to reduce the effect of velocity changes on the plateau concentration.

Sodium Hydroxide / Ammonium Nitrate Systems

In the case of the sodium hydroxide / ammonium nitrate

systems, the effluent response was quite different than that observed in the ammonium hydroxide systems. The plots from these runs are shown in Figures 26, 27, and 28. First of all, the nitrate ions pass through the column without reacting with the solid surface. Nonreacting species travel at the frontal advance rate frequently called the indifferent or salinity wave and with dimensionless velocity (ξ / τ) of one since solution electroneutrality must be maintained. Therefore, an equal number of cations and anions must migrate simultaneously.

The quartz surface is a weak cation exchanger which will establish equilibrium with the three cations present in the solution: hydrogen, ammonium, and sodium. As this is a high pH system, the formation of sodium sites will be favored. Hence, the advance rate of sodium ions through the column will be delayed as they exchange for either hydrogen or ammonium ions. When either a hydrogen or ammonium ion is released from the solid surface during the exchange reaction, the hydroxide ions in the system are consumed by Equation (4) or (5) as written earlier creating a delay in the pH response. Equation (6) is utilized and a similiar expression is written for each of the various species which will exist in the column solutions (Bunge and Radke, 1985):

$$\frac{\partial C_{Na}}{\partial t} + \rho_s \frac{(1-\epsilon)}{\epsilon} \frac{\partial n_{Na}}{\partial t} + \frac{u}{\epsilon} \frac{\partial C_{Na}}{\partial z} = 0 \tag{22}$$

$$\frac{\partial C_H}{\partial t} + \rho_s \frac{(1-\epsilon)}{\epsilon} \frac{\partial n_H}{\partial t} + \frac{u}{\epsilon} \frac{\partial C_H}{\partial z} = r_H \tag{23}$$

$$\frac{\partial C_A}{\partial t} + \rho_s \frac{(1-\epsilon)}{\epsilon} \frac{\partial n_A}{\partial t} + \frac{u}{\epsilon} \frac{\partial C_A}{\partial z} = r_A \tag{24}$$

$$\frac{\partial C_{OH}}{\partial t} + \frac{u}{\epsilon} \frac{\partial C_{OH}}{\partial z} = r_{OH} \tag{25}$$

$$\frac{\partial C_N}{\partial t} + \frac{u}{\epsilon} \frac{\partial C_N}{\partial z} = 0 \tag{26}$$

$$\frac{\partial C_{AmOH}}{\partial t} + \frac{u}{\epsilon} \frac{\partial C_{AmOH}}{\partial z} = -r_A \tag{27}$$

where Na is the sodium ion, H is the hydrogen ion, A is the ammonium ion, OH is the hydroxide ion, N is the nitrate ion, AmOH is undissociated ammonium hydroxide and n_i is the amount of the particular species exchanged. In addition to cation exchange, hydrogen, hydroxide, and ammonium ions are also consumed by their respective neutralization reactions (Equations (4) and (5)) which will require that $r_{OH}=r_A + r_H$. Therefore, Equations (23) through (25) and (27) can be combined to eliminate some of the unknown reaction rates yielding two differential equations:

$$\frac{\partial(C_A - C_H - C_{OH})}{\partial t} + \rho_s \frac{(1-\epsilon)}{\epsilon} \frac{\partial(n_A + n_H)}{\partial t} + \frac{u}{\epsilon} \frac{\partial(C_A + C_H - C_{OH})}{\partial z} = 0 \qquad (28)$$

$$\frac{\partial(C_A + C_{AmOH})}{\partial t} + \rho_s \frac{(1-\epsilon)}{\epsilon} \frac{\partial n_A}{\partial t} + \frac{u}{\epsilon} \frac{\partial(C_A + C_{AmOH})}{\partial z} = 0 \qquad (29)$$

Next, it is assumed that the three cation exchange reactions are described by mass-action expressions:

$$MH + Na^+ = MNa + H^+ \qquad (30)$$

$$K_1 = \frac{n_{Na} C_H}{n_H C_{Na}} \qquad (31)$$

$$MH + NH_4^+ = MNH_4 + H^+ \qquad (32)$$

$$K_2 = \frac{n_A C_H}{n_H C_A} \qquad (33)$$

The exchange between the sodium and ammonium ions will be found by subtracting Equations (30) and (32). Lastly, it is necessary to impose exchange site conservation, solution electroneutrality, and total ammonia conservation:

$$n_{tot} = n_H + n_{Na} + n_A \qquad (34)$$

$$C_{OH} + C_N = C_H + C_{Na} + C_A \qquad (35)$$

$$C_{Tot,Am} = C_A + C_{AmOH} \tag{36}$$

where $C_{Tot,Am}$ is the total ammonia in the system. This system is now fully specified by Equations (22), (28), (29), (31), (33), (34), (35), and (36). In this case, the system is bivarient (Helferrich and Klein, 1970; and Vislocky, 1982) which will generate a single indifferent wave traveling with a dimensionless velocity of one followed by two exchanging waves. At any given point across the indifferent wave $\Delta n_H = \Delta n_A = \Delta n_{Na} = 0$. The species velocities of the ion exchange waves are shown below:

$$\left.\frac{d\xi}{d\tau}\right|_{C_{Na}} = \frac{1}{1+\rho_s\frac{(1-\epsilon)}{\epsilon}\frac{dn_{Na}}{dC_{Na}}} \tag{37}$$

$$\left.\frac{d\xi}{d\tau}\right|_{(C_A+C_H-C_{OH})} = \frac{1}{1+\rho_s\frac{(1-\epsilon)}{\epsilon}\frac{d(n_A+n_H)}{d(C_A+C_H-C_{OH})}} \tag{38}$$

$$\left.\frac{d\xi}{d\tau}\right|_{(C_A+C_{AmOH})} = \frac{1}{1+\rho_s\frac{(1-\epsilon)}{\epsilon}\frac{dn_A}{d(C_A+C_{AmOH})}} \tag{39}$$

Applying coherence (Helferrich and Klein, 1970) dictates

that variation in the concentration profiles of one of the species must include compensating variations in the concentrations of the other waves. In addition, the velocity of the concentration wave for one species must be equal to that of the others. The solution to this particlar set of equations is the subject of another research project.

Chapter 6

CONCLUSIONS AND RECOMMENDATIONS

Column leaching of zinc oxide showed that chromatographic phenomena can contribute to the zinc production rate. For leaching solutions with large concentrations of ammonium hydroxide, effluent zinc concentrations gradually increases to a plateau value. A simple chromatographic model suggests that adsorption of the dissolved zinc will explain this observation.

For solutions of sodium hydroxide and ammonium nitrate, zinc concentration peaks ahead of the delayed high pH response. The decline in zinc concentration at higher pH is probably tied to the decrease of ammonium ions in this solution. The approach needed to describe the responsible ion exchange contributions is outlined.

Flow effects on the zinc concentration in the effluent did not yield conclusive results. Although some slight difference in plateau levels was noted, it was not consistent in either direction, i.e., lower plateau for a higher flow rate. This might be expected since increasing the velocity and thereby decreasing the residence time is offset by the corresponding increase of the mass transfer coefficient.

The chromatographic phemonena of both the solubilized zinc and ammonia solutions should be studied further. Zinc adsorption should be measured to confirm whether the suspected concave up isotherm is correct. Ion exchange chromatography by weakly dissociable salts of weak acid sites has not been explored experimentally or theoretically before. This research suggests that this combination of chemistry can provoke unusual phenomena which should be quantified further.

The system examined in this project utilized relatively simple chemistry. However, applicability toward actual use is somewhat limited. Therefore, examination of either a zinc sulfide or copper sulfide system might be in order. Both of these systems have been subjected to earlier investigation and a wealth of data (kinetic and otherwise) exists. Once this work has been completed, investigation of actual sulfide ore systems could be initiated.

NOMENCLATURE

C = concentration of solute in solution
C_s = zinc solubility limit for the leachant
d_p = average particle diameter
k_e = external mass transfer coefficient
K = adsorption constant (Langmuir)
L = column length
n = concentration of solute adsorbed on solid surface
n_{max} = maximum concentration of solute which can be adsorbed on the solid
PV = pore volume
r = rate of production of adsorbing solute
Sc = Schimdt Number
t = time
u = superficial velocity
z = axial position

Greek
α = constant
γ = Damköhler Number
Γ = dimensionless concentration (adsorbed on solid surface)
ϵ = void fraction
θ = dimensionless concentration (solute concentration in solution)
ν = kinematic viscosity
ξ = dimensionless position
ρ_s = solid density
τ = dimensionless time

REFERENCES

Bunge, A.L. and Radke, C.J., "The Origin of Reversible Hydroxide Uptake on Reservoir Rock," Soc. Pet. Eng. J., 25, 711-718 (1985).

Carnahan, T.G., "Effects of Temperature On Simulated In-Situ Leaching of a Chalcopyrite Ore.", U.S. Department of the Interior, Bureau of Mines, Washington D.C. (1982).

Carnahan, T.G. and Lindstrom, R.F., "Effects of Sodium Chloride Leach Solution Additive on Simulated In-Situ Leaching of a Chalcopyrite Ore.", U.S. Department of the Interior, Bureau of Mines, Washington D.C. (1982).

Dutrizac, J.E. and MacDonald, R.J.C., "The Dissolution of Sphalerite in Ferric Chloride Solutions", Metall. Trans. 9B, 543-551 (1970).

Gluekauf E., "Theory of Chromatography. Part VI. Precision Measurements of Adsorption and Exchange Isotherms from Column-Elution Data," J. Chem. Soc., 3280 (1949).

Goddard, J.B. and Brosnahan, D.R., "Rate of Consumption of Dissolved Oxygen During Ammonium Carbonate In-Situ Leaching of Uranium", Mining Eng. 34, 1589-1596 (1982).

Helfferich, F. and Klein, G., Multicomponent Chomotography, Marcel Dekker, New York (1970)

Habib, Jr. E.T. and Vogt, J.C., "Process for the In-Situ Leaching of Uranium", Mobil Oil Corporation, U.S. Patent: 4,312,840, July 28,1978.

Jones, H.C. and Klaman, C.A., "Zinc Oxide in Latex II-The Influence of Zinc Oxide on Collidal Stability.", Rubber Age 73, 67-70 (1953).

Litz, L.M., "In-Situ Uranium Mining with Oxygen", Mining Eng. 34, 52-56 (1982)

Martin, B., Interox Chemicals Limited, U.S. Patent: 4,344,923, October 21, 1978.

Nigbor, M.T., Englemann, W.H., and Tweeton, D.R., "Case History of a Pilot Scale Acidic In-Situ Uranium Leaching Experiment.", U.S. Department of the Interior, Bureau of Mines, Washington D.C. (1982).

Paul, J.M., Johnson, W.F., Fletcher, A., Venuto, P.B.,"In-Situ Leaching of South Texas Uranium Ores. II. Oxidative Removal of Adsorbed Ammonium Ions with Sodium Hypochlorite" paper SPE 10232 presented at 1981 SPE Annual Exhibition, San Antonio, Texas, Oct. 5-7, 1981

Schafer, J.L., White, M.L., and Caenepeel, C.E., "Application of the Shrinking Core Model for Copper Oxide Leaching.", Mining Eng. 31, 165-171 (1979)

Sherwood, T.K., Pigford, R.L. and Wilke, C.R., Mass Transfer, Chapter 6, McGraw Hill, New York (1975)

Thomas, B.K. and Fray, D.J., "Leaching of Oxidic Zinc Materials with Chlorine and Chlorine Hydrate.", Metall. Trans. 12B, 281-285 (1981)

Venkataswamy, Y. and Khangaonkar, P.R., "Ferric Chloride Leaching of Sphalerite in the Presence of an Organic Solvent for Sulfur.", Hydrometallurgy, 7, 1-5 (1981)

Vislocky, J.M., "Local Equilibrium Theory for Bivarient Fixed-Bed Sorption Systems," Ph.D Thesis, University of California, Berkley (1982)

Vogt, T.C., Strom, E.T., Dixon, S.A., Johnson, W.F., and Venuto, P.B., "In-Situ Leaching of Crownpoint, NM, Uranium Ore-2. Laboratory Study of a Mild Leaching System.", Soc. Pet. Eng. J. 22, 1013-1032 (1982).

Wagman, et al., NBS Tables of Chemical Thermodynamic Properties, J. Phys. Chem. Ref. 11, Supplement #2 (1982).

Walsh, M.P., Schecheter,R.S., and Humeneck, M.J., AIME National Meeting, New Orleans, LA, Soc. Mining Eng. (pamphlet) 99-111 (1979).

APPENDIX

Zinc Species Distribution Calculation

The following species are formed when zinc is dissolved in an aqueous solution (from Wagman et al. 1982): $Zn(OH)_2$, Zn^{2+}, $ZnOH^+$, $HZnO_2^-$, and ZnO_2^{2-}. Assuming mass action and neglecting activity effects, the following equations and corresponding equilibrium expressions can be written for the dissociation and formation of the various ions in solution:

$$Zn(OH)_2 = Zn^{2+} + 2OH^- \quad , \quad K_1 = \frac{[Zn^{2+}]\,[OH^-]^2}{[Zn(OH)_2]} \qquad (A1)$$

$$Zn(OH)_2 = ZnOH^+ + OH^- \quad , \quad K_2 = \frac{[ZnOH^+]\,[OH^-]}{[Zn(OH)_2]} \qquad (A2)$$

$$ZnOH^+ = Zn^{2+} + OH^- \quad , \quad K_3 = \frac{[Zn^{2+}]\,[OH^-]}{[ZnOH^+]} \qquad (A3)$$

$$Zn(OH)_2 = HZnO_2^- + H^+ \quad , \quad K_4 = \frac{[HZnO_2^-]\,[H^+]}{[Zn(OH)_2]} \qquad (A4)$$

$$HZnO_2^- = ZnO_2^{2-} + H^+ \quad , \quad K_5 = \frac{[ZnO_2^{2-}]\,[H^+]}{[HZnO_2^-]} \qquad (A5)$$

$$Zn(OH)_2 = ZnO_2^{2-} + 2H^+ \quad , \qquad K_6 = \frac{[ZnO_2^{2-}]\,[H^+]^2}{[Zn(OH)_2]} \qquad (A6)$$

By making a balance of the total zinc in solution, it is possible to calculate the fraction of each particular species in solution.

$$[ZnT] = [Zn^{2+}] + [ZnOH^+] + [HZnO_2^-] + [ZnO_2^{2-}] + [Zn(OH)_2] \qquad (A7)$$

Incorporating Equations (A1) through (A6) and that of water dissociation into Equation (A7), it is possible to derive an expression for the neutral zinc fraction of the total zinc as a function of the hydroxide ion concentration:

$$\frac{[Zn(OH)_2]}{[ZnT]} = \frac{1}{\frac{K_1}{[OH^-]} + \frac{K_2}{[OH^-]} + K_4\frac{[OH^-]}{K_W} + K_6\frac{[OH^-]}{K_W} + 1} \qquad (A8)$$

The fraction of the total zinc which is in the various ionic forms is easily calculated from the appropriate equilibria combined with Equation (A8).

Equilibrium constants for Equations (A1) through (A6) are calculated from the Gibbs free energy of reaction, $K=\exp(-\Delta G_{rxn}/RT)$. For the species in question, the values

for the Gibbs free energy of formation at a temperature of 25 C are shown in Table A1 (from Wagman, et al.). The values of the ΔG_{rxn} and the equilibrium constants for a temperature of 25 C are shown in Table A2.

A computer program was written to calculate zinc species as a function of pH. This program is shown in Table A3. The species curves generated are shown in Figure 2.

With the addition of NH_4OH, NH_4NO_3, and/or NaOH, more species will exist: NH_4OH, NH_4^+, NO_3^-, Na^+, $ZnNH_3^{2+}$, $Zn(NH_3)_2^{2+}$, and $Zn(NH_3)_3^{2+}$. Equilibrium expressions written for these additional species are shown below.

$$NH_4OH = NH_4^+ + OH^- , \quad K_B = \frac{[NH_4^+]\,[OH^-]}{[NH_4OH]} \qquad (A9)$$

$$NH_4NO_3 = NH_4^+ + NO_3^- , \quad \text{total dissociation} \qquad (A10)$$

$$NaOH = Na^+ + OH^- , \quad \text{total dissociation} \qquad (A11)$$

$$Zn^{2+} + NH_4^+ = ZnNH_3^{2+} + H^+, \; K_7 = \frac{[H^+]\,[ZnNH_3^{2+}]}{[Zn^{2+}]\,[NH_4^+]} \qquad (A12)$$

Table A1

Gibbs Free Energy of Formation for Zinc Species at 25 C

(From Wagman, et al. 1982)

Species	ΔG(kJ/mol)
$[H^+]$	0.0000
$[OH^-]$	-157.35
$[Zn(OH)_2]$	-522.73
$[Zn^{2+}]$	-147.06
$[HZnO_2^-]$	-457.08
$[ZnOH^+]$	-330.10
$[ZnO_2^{2-}]$	-384.24

Table A2

Equilibrium Constants for Zinc Species at 25 C

Reaction	Equilibrium Constant	ΔG_{rxn}(kJ/mol)
(A1)	$K_1=2.05 \times 10^{-11}$	60.97
(A2)	$K_2=6.54 \times 10^{-07}$	35.28
(A4)	$K_4=3.11 \times 10^{-12}$	65.65
(A6)	$K_6=5.30 \times 10^{-25}$	138.49
water	$K_W=1.00 \times 10^{-14}$	-

Table A3

Fortran Program Used to Generate Zinc Species Distribution as a Function of pH

```
C       CALCULATION OF ZN SPECIES
C       EQUILIBRIUM CONSTANTS
        REAL K1, K2, K4, K6, KW
        K1=2.05 E-11
        K2=6.54 E-07
        K4=3.11 E-12
        K6=5.30 E-25
        KW=1.00 E-14
C       INTIALIZE PH,KOUNTER
        KOUNT=0
        PH=1.00
10      H=10**(-PH)
        OH=KW/H
        ZNOH2=1/(K1/(OH**2)+(K2/OH)+(K4/KW)*OH+K6*(OH**2)/(KW**2)+1
        ZN=K1*ZNOH2/(OH**2)
        ZNOH=K2*ZNOH2/OH
        HZNO2=(K4*ZNOH2)/H
        ZNO2=K6*ZNOH2/H**2
        IF(PH.GE.14)GOTO 30
        WRITE(19,1) PH,ZNOH2
        WRITE(20,1)PH,ZN
        WRITE(21,1)PH,ZNOH
        WRITE(22,1)PH,HZNO2
        WRITE(23,1)PH,ZNO2
        KOUNT=KOUNT +1
        PH=PH+0.02
        IF(KOUNT.EQ.50)GOTO 20
        GOTO 10
20      WRITE(4,2) PH,ZNOH2,ZN,ZNOH,HZNO2,ZNO2
        KOUNT=0
        GOTO 10
1       FORMAT(1X,F5.2,6X,F7.5)
2       FORMAT(1X,F5.2,5X,F7.5,5X,F7.5,5X,F7.5,5X,F7.5,5X,F7.5)
30      END
```

$$Zn^{2+} + 2NH_4^+ = Zn(NH_3)_2^{2+} + 2H^+ \quad K_8 = \frac{[Zn(NH_3)_2^{2+}][H^+]^2}{[Zn^{2+}][NH_4^+]^2} \quad (A13)$$

$$Zn^{2+} + 3NH_4^+ = Zn(NH_3)_3^{2+} + 3H^+ \quad K_9 = \frac{[Zn(NH_3)_3^{2+}][H^+]^3}{[Zn^{2+}][NH_4^+]^3} \quad (A14)$$

With the additional species NO_3^-, NH_4^+, and NH_4NO_3, three equations are now required to calculate the zinc distribution: total zinc balance, a total ammonia balance, and an electroneutrality balance of the species. The total zinc balance is changed only slightly from before because of the complexing now possible with the ammonia.

$$[ZnT] = [Zn^{2+}] + [ZnOH^+] + [HZnO_2^-] + [ZnO_2^{2-}] + [Zn(OH)_2] + [ZnNH_3^{2+}] + [Zn(NH_3)_2^{2+}] + [Zn(NH_3)_3^{2+}] \quad (A15)$$

$$[AmmT] = [NH_4^+] + [NH_4OH] + [ZnNH_3^{2+}] + 2[Zn(NH_3)_2^{2+}] + 3[Zn(NH_3)_3^{2+}] \quad (A16)$$

$$[H^-] + 2[Zn^{2+}] + [ZnOH^+] + 2[ZnNH_3^{2+}] + 2[Zn(NH_3)_2^{2+}] + 2[Zn(NH_3)_3^{2+}] + [NH_4^+] + [Na^+] = [OH^-] + [HZnO_2^-] + 2[ZnO_2^{2-}] + [NO_3^-] \quad (A17)$$

By using the Equations (A1) through (A14), substitutions can be made for some of the species. These expressions are

then substituted in Equations (A15) through (A17) to give the resulting equations:

$$\frac{[ZnT]}{[Zn(OH)_2]} = \frac{K_1}{[OH^-]^2} + \frac{K_2}{[OH^-]} + \frac{K_4}{[H^+]} + \frac{K_6}{[H^+]^2} + 1 + \frac{K_1 K_7}{K_W}\frac{[NH_4^+]}{[OH^-]} + \frac{K_1 K_8 [NH_4^+]^2}{K_W^2} + \frac{K_1 K_9}{K_W^2}\frac{[NH_4^+]^3}{[H^+]} \quad (A18)$$

$$\frac{[AmmT]}{[NH_4^+]} = 1 + \frac{[OH^-]}{K_B} + \frac{K_1 K_7}{K_W}\frac{[Zn(OH)_2]}{[OH^-]} + 2\frac{K_1 K_8 [Zn(OH)_2][NH_4^+]}{K_W^2} + 3\frac{K_1 K_9 [Zn(OH)_2][NH_4^+]^2}{K_W^2 [H^+]} \quad (A19)$$

$$[H^+] + [Na^+] + [NH_4^+] + 2\,K_1\,\frac{[Zn(OH)_2]}{[OH^-]^2} + K_2\,\frac{[Zn(OH)_2]}{[OH^-]}$$

$$+ \frac{2\,K_1\,K_7}{K_W}\,\frac{[Zn(OH)_2][NH_4^+]}{[OH^-]} + \frac{2\,K_1\,K_8\,[Zn(OH)_2][NH_4^+]^2}{K_W^2}$$

$$+ \frac{2\,K_1\,K_9}{K_W^2}\,\frac{[Zn(OH)_2][NH_4^+]^3}{[H^+]} = [OH^-] + [NO_3^-] +$$

$$K_4\,\frac{[Zn(OH)_2]}{[H^+]} + 2\,K_6\,\frac{[Zn(OH)_2]}{[H^+]^2} \qquad \text{(A20)}$$

As before, equilibrium constants were calculated from the Gibbs free energy of formation. The Gibbs free energy and the associated equilibrium constants are shown in Table A4. Using equations (A1) through (A6), (A9), (A12) through (A14) and (A18) through (A20), the species distribution is obtained. These equations are solved simultaneously using the program shown in Table A5.

Table A4

Gibbs Free Energy of Formation and Equilibrium Constants for Zinc Ammonia Complexes at 25 C

Species	ΔG (kJ/mol)	K
$ZnNH_3^{2+}$	-185.7	6.88×10^{-08} (A12)
$Zn(NH_3)_2^{2+}$	-225.0	6.18×10^{-15} (A13)
$Zn(NH_3)_3^{2+}$	-264.3	5.55×10^{-22} (A14)
ammonia	-	1.80×10^{-05} (A9)

Table A5

Program to Calculate Zinc Species Distribution with Ammonium Hydroxide, Ammonium Salt, and/or Sodium Hydroxide in Solution

```
150 '   npara   the number of parameters
160 '   nresid  the number of residuals, ie., the number of residual terms in
165 '           the sum-of-squares function
170 READ NPARA,NRESID
171 DATA 11,11
174 'PRINT NPARA, NRESID
175 'STOP
180 '
190 NSIZE=NPARA*(NPARA +1)\2
191 'PRINT NSIZE
192 'STOP
200 DIM A(NSIZE),C(NSIZE),B(NPARA),X(NPARA),V(NPARA),D(NPARA),F(NRESID)
210 '
220 'read starting values of the parameters
230 FOR I=1 TO NPARA: READ B(I):NEXT
231 DATA 1. E-02,1. E-02, 1. E-02, 1. E-02,1. E-02, 1. E-02, 1. E-02, 1. E-02,1. E-02,1. E-02, 1. E-02
232 'FOR I=1 TO NPARA: PRINT B(I):NEXT
233 'STOP
240 '
250 '
260 GOTO 3020   'detour around subroutines
1205 IF I=1 GOTO 1240
1206 IF I=2 GOTO 1252
1207 IF I=3 GOTO 1254
1208 IF I=4 GOTO 1256
1209 IF I=5 GOTO 1258
1210 IF I=6 GOTO 1260
1211 IF I=7 GOTO 1262
1212 IF I=8 GOTO 1264
1213 IF I=9 GOTO 1266
1214 IF I=10 GOTO 1268
1215 IF I=11 GOTO 1270
1216 'IF I=12 GOTO 1272
1240 F(1)=2.05E-11*(B(1)/B(2)^2)-B(3)
1245 GOTO 1296
1252 F(2)=6.54E-07*B(1)/B(2)-B(4)
1253 GOTO 1296
1254 F(3)=311!*B(1)*B(2)-B(5)
1255 GOTO 1296
1256 F(4)=5300!*B(1)*B(2)^2-B(6)
1257 GOTO 1296
1258 F(5)=.000141*B(1)*B(11)/B(2)-B(7)
1259 GOTO 1296
1260 F(6)=1266.9*B(1)*B(11)^2-B(8)
1261 GOTO 1296
1262 F(7)=1.14E+12*B(1)*B(11)^3*B(2)-B(9)
1263 GOTO 1296
1264 F(8)=B(11)*B(2)/.000018-B(10)
```

Table A5
(continued)

```
1265 GOTO 1296
1266 F(9)=B(3)+B(4)+B(5)+B(6)+B(1)+B(7)+B(8)+B(9)-.000306
1267 GOTO 1296
1268 F(10)=B(11)+B(10)+B(7)+2*B(8)+3*B(9)-.155
1269 GOTO 1296
1270 F(11)=B(2)+B(5)+2*B(6)+.005-1E-14/B(2)-2*B(3)-B(4)-2*B(7)-2*B(8)-2*B(9)-B(11)
1271 GOTO 1296
1272 'F(12)=1E-14-B(2)*B(12)
1296 P=P+F(I)*F(I)
1297 'PRINT F(I):NEXT
1298 'STOP
1299 NEXT I:RETURN
1300 '
1320 '
1340 '
1360 'DERIVATIVE EVALUATION SUBROUTINE, derivative of f(i) wrt B(1,...,NPARA)
1380 '  returns vector d() a function of residual i and parameters b()
1381 FOR L=1 TO 11
1382 D(L)=0#
1383 NEXT L
1384 IF I=1 GOTO 1400
1386 IF I=2 GOTO 1404
1387 IF I=3 GOTO 1408
1388 IF I=4 GOTO 1412
1389 IF I=5 GOTO 1416
1390 IF I=6 GOTO 1421
1391 IF I=7 GOTO 1426
1392 IF I=8 GOTO 1431
1393 IF I=9 GOTO 1435
1394 IF I=10 GOTO 1439
1395 IF I=11 GOTO 1445
1396 'IF I=12 GOTO 1456
1400 D(1)=2.05E-11/B(2)^2
1401 D(2)=-2*2.05E-11*B(1)/B(2)^3
1402 D(3)=-1#
1403 GOTO 1460
1404 D(1)=6.54E-07/B(2)
1405 D(2)=-6.54E-07*B(1)/B(2)^2
1406 D(4)=-1#
1407 GOTO 1460
1408 D(1)=311!*B(2)
1409 D(5)=-1#
1410 D(2)=311!*B(1)
1411 GOTO 1460
1412 D(1)=5300!*B(2)^2
1413 D(6)=-1#
1414 D(2)=2*5300!*B(1)*B(2)
1415 GOTO 1460
1416 D(1)=.000141*B(11)/B(2)
1417 D(7)=-1#
1418 D(11)=.000141*B(1)/B(2)
1419 D(2)=-.000141*B(1)*B(11)/B(2)^2
1420 GOTO 1460
1421 D(1)=1266.9*B(11)^2
1422 D(8)=-1#
1423 D(11)=1266.9*B(11)*2*B(1)
1425 GOTO 1460
1426 D(1)=1.14E+12*B(11)^3*B(2)
1427 D(9)=-1#
1428 D(11)=1.14E+12*3*B(1)*B(11)^2*B(2)
```

Table A5
(continued)

```
1429 D(2)=1.14E+12#B(1)#B(11)^3
1430 GOTO 1460
1431 D(2)=B(11)/.000018
1432 D(10)=-1
1433 D(11)=B(2)/.000018
1434 GOTO 1460
1435 D(1)=1#
1436 D(3)=1#:D(4)=1#:D(5)=1#:D(6)=1#:
1437 D(7)=1#:D(8)=1#:D(9)=1#
1438 GOTO 1460
1439 D(7)=1#
1440 D(8)=2#
1441 D(9)=3#
1442 D(10)=1#
1443 D(11)=1#
1444 GOTO 1460
1445 D(2)=1#+1E-14/B(2)^2
1446 D(3)=-2#
1447 D(4)=-1#
1448 D(5)=1#
1449 D(6)=2#
1450 D(7)=-2#
1451 D(8)=-2#
1452 D(9)=-2#
1453 D(11)=-1#
1455 GOTO 1460
1456 'D(2)=-B(12)
1457 'D(12)=-B(2)
1460 RETURN
1480 '
1500 '################################################################################
3000 '
3010 '
3020 PRINT :PRINT :PRINT :PRINT "Modified Marquardt Procedure for Minimizing Nonlinear Sum of Squares":
PRINT
3030 '
3040 STIME$=TIME$
3050 TOL=EPS          'on underflow Marquardt parameter is set to TOL
3060 FINCRE=10!       'increase factor
3070 FDECRE=.4        'decrease factor
3080 FACTR=.0001      'the Marquardt parameter, initial value
3090 PHI=1            'quantity used to control singularity
3100 IFNCT=0: IDERCT=0    'count of function and derivative evaluations
3110 '
3120 IFNCT=IFNCT+1:GOSUB 1200'  COMPUTE THE RESIDUALS F(1,....,NRESID
3121 'AND THEIR SUM OF SQUARES P
3125 'FOR I=1 TO NRESID:PRINT F(I):NEXT I
3126 'STOP
3130 '
3140 'top of the iteration
3150 '
3160 IDERCT=IDERCT+1:FACTR=FACTR#FDECRE:P0=P:PRINT USING "Iteration=###";IDERCT;:PRINT TAB(18);:PRINT
USING "Sum of Squares= #.########^^^^";P0;:PRINT TAB(52):PRINT USING "M Factor= #.#####^^^^";FACTR
3170 FOR J=1 TO NSIZE: A(J)=0: NEXT J:  FOR J=1 TO NPARA: V(J)=0: NEXT J
```

Table A5
(continued)

```
3180 FOR I=1 TO NRESID
3181 'PRINT NRESID
3182 'STOP
3190 GOSUB 1360   'Compute  D(1,0!0!0!,NPARA) THE DERIVATIVES OF F(I) WRT B()
3195 'PRINT D(1),D(2),D(3),D(4),D(5),D(6),D(7),D(8),D(9),D(10),D(11),D(12)
3196 'PRINT"These are the respectives derivitives for each F(I)"
3197 'STOP
3200     FOR J=1 TO NPARA: V(J)=V(J) + D(J)*F(I):NQ=J*(J-1)/2:FOR K=1 TO J:A(NQ+K)=A(NQ+K)+D(J)*D(K):NEXT
K,J,I
3201 'STOP
3210 '
3220 '
3230 FOR J=1 TO NSIZE:C(J)=A(J):NEXT J:  FOR J=1 TO NPARA:D(J)=B(J):NEXT J
3231 'PRINT"These are the current B(I)'s"
3232 'FOR L=1 TO NPARA:PRINT B(L):NEXT L
3233 'STOP
3235 'PRINT"THESE ARE THE NEW D(L)"
3236 'FOR L=1 TO NPARA:PRINT D(L):NEXT L
3237 'STOP
3240 '


3260 FOR J=1 TO NPARA: NQ=J*(J+1)/2: A(NQ)=C(NQ)+(C(NQ)+PHI)*FACTR:X(J)=-V(J):IF J>1 THEN FOR I=1 TO J-1:A(
NQ-I)=C(NQ-I):NEXT I
3270 NEXT J
3271 'FOR L=1 TO NSIZE:PRINT A(L):NEXT
3272 'STOP
3280 '
3290 'PRINT "chol dec":'Choleski decomposition of A()
3300 FOR J=1 TO NPARA:NQ=J*(J+1)/2: IF J=1 THEN 3310 ELSE FOR I=J TO NPARA:M=I*(I-1)/2+J:S=A(M):FOR K=1 TO
J-1:S=S-A(M-K)*A(NQ-K):NEXT K:A(M)=S:NEXT I
3310 IF A(NQ)<=0 THEN 3420 ELSE S=FNSQRT(A(NQ)):FOR I=J TO NPARA:M=I*(I-1)/2+J:A(M)=A(M)/S:NEXT I,J
3312 'SOMETIMES EXIT FROM INSIDE J-LOOP
3320 'PRINT "Back substitution"
3330 X(1)=X(1)/A(1):IF NPARA=1 THEN 3370
3340 NQ=1:FOR I=2 TO NPARA:FOR J=1 TO I-1:NQ=NQ+1:X(I)=X(I)-A(NQ)*X(J):NEXT J:NQ=NQ+1:X(I)=X(I)/A(NQ):NEXT
I
3341 'FOR I=NPARA TO 2 STEP -1:NQ=I*(I-1)/2
3342 'PRINT NQ
3343 'STOP
3344 'NEXT I
3350 X(NPARA)=X(NPARA)/A(NSIZE):FOR I=NPARA TO 2 STEP -1:NQ=I*(I-1)/2:FOR J=1 TO I-1:X(J)=X(J)-X(I)*A(NQ+J)
:NEXT J:X(I-1)=X(I-1)/A(NQ):NEXT I
3351 FOR L=1 TO NARPA:PRINT X(L):NEXT
3352 'STOP
3360 '
3361 'FOR L=1 TO NPARA:PRINT X(L):NEXT
3362 'STOP
3370 NCT=0:FOR I=1 TO NPARA:B(I)=D(I)+X(I):IF B(I)=D(I) THEN NCT=NCT+1
```

Table A5
(continued)

```
3380 NEXT I:IF NCT=NPARA THEN GOTO 3470
3390 '
3400 IFNCT=IFNCT+1:GOSUB 1200 ':PRINT "ifnct=";IFNCT;"ss=";P
3401 'compute F() and P  sum of squares
3406 ' PRINT P
3407 ' STOP
3408 'PRINT P0
3409 'STOP
3410 IF P<P0 THEN 3160
3420 FACTR=FACTR#FINCRE: IF FACTR=0 THEN FACTR=TOL
3430 GOTO 3260
3440 '
3450 '
3460 '
3470 PRINT :PRINT "Converged Solution";
3480 PRINT TAB(30);"Sum of Squares=";:PRINT USING " #.#####^^^^";P0:PRINT
3490  COLOR 15,0:PRINT "Parameters= ":FOR I=1 TO NPARA:PRINT USING "  +#.######^^^^ ";B(I);:NEXT I:PRINT:
COLOR 7,0
3500 PRINT :PRINT "Iteration count= ";IDERCT;" Evaluation Count="IFNCT
3510 PRINT:PRINT DATE$;"    start time=";STIME$;"Finish time=";TIME$
3520 END
```